bioRxiv preprint doi: https://doi.org/10.1101/151340; this version posted June 20, 2017. The copyright holder for this preprint (which was not certified by peer review) is the author/funder, who has granted bioRxiv a license to display the preprint in perpetuity. It is made available under aCC-BY-NC-ND 4.0 International license.

Increased ParB level affects expression of stress response, adaptation and virulence operons and potentiates repression of promoters adjacent to the high affinity binding sites *parS3* and *parS4* in *Pseudomonas aeruginosa*

Adam Kawałek[1], Krzysztof Głąbski[1], Aneta Agnieszka Bartosik[1], Anna Fogtman[2] and Grażyna Jagura-Burdzy[1]*

[1] Institute of Biochemistry and Biophysics, Polish Academy of Sciences, Department of Microbial Biochemistry, Warsaw, Poland

[2] Institute of Biochemistry and Biophysics, Polish Academy of Sciences, Laboratory of Microarray Analysis, Warsaw, Poland

bioRxiv preprint doi: https://doi.org/10.1101/151340; this version posted June 20, 2017. The copyright holder for this preprint (which was not certified by peer review) is the author/funder, who has granted bioRxiv a license to display the preprint in perpetuity. It is made available under aCC-BY-NC-ND 4.0 International license.

Abstract

Similarly to its homologs in other bacteria, *Pseudomonas aeruginosa* partitioning protein ParB facilitates segregation of newly replicated chromosomes. Lack of ParB is not lethal but results in increased frequency of anucleate cells production, longer division time, cell elongation, altered colony morphology and defective swarming and swimming motility. Unlike in other bacteria, inactivation of *parB* leads to major changes of the transcriptome, suggesting that, directly or indirectly, ParB plays a role in regulation of gene expression in this organism.

ParB overproduction affects growth rate, cell division and motility in a similar way as ParB deficiency. To identify primary ParB targets, here we analysed the impact of a slight increase in ParB level on *P. aeruginosa* transcriptome. ParB excess, which does not cause changes in growth rate and chromosome segregation, significantly alters the expression of 176 loci. Most notably, the mRNA level of genes adjacent to high affinity ParB binding sites *parS1-4* close to *oriC* is reduced. Conversely, in cells lacking either *parB* or functional *parS* sequences the orfs adjacent to *parS3* and *parS4* are upregulated, indicating that direct ParB-*parS3/parS4* interactions repress the transcription in this region. In addition, increased ParB level brings about repression or activation of numerous genes including several transcriptional regulators involved in SOS response, virulence and adaptation. Overall, our data support the role of partitioning protein ParB as a transcriptional regulator in *Pseudomonas aeruginosa*.

bioRxiv preprint doi: https://doi.org/10.1101/151340; this version posted June 20, 2017. The copyright holder for this preprint (which was not certified by peer review) is the author/funder, who has granted bioRxiv a license to display the preprint in perpetuity. It is made available under aCC-BY-NC-ND 4.0 International license.

Introduction

Accurate copying and segregation of genetic material to progeny cells is crucial for survival and maintenance of species identity. The process of bacterial DNA segregation was first deciphered for low-copy-number plasmids [1–4]. Active partitioning of such plasmids during cell division requires three specific plasmid-encoded factors: an NTPase (A-component), a DNA-binding protein (DBP, B-component) and a special site in DNA, designated centromere-like sequence (*parS*/*parC*). Interactions of DBP with *parS* sequence(s) lead to formation of segrosomes which are then separated by a dynamic NTPase machinery to polar positions assuring their proper segregation during the subsequent cell division [2,3]. Plasmidic active partition systems have been classified into three groups based on the type of NTPase and structure of DBP [2,4]. Homologs of plasmidic Type IA partition proteins, Walker-type ATPases (ParAs) and large DBPs with helix-turn-helix motifs (ParBs), which after binding to *parS* spread on DNA and form large nucleoprotein complexes [5], are also encoded on the majority of bacterial chromosomes [3,4,6]. Multiple copies of highly conserved *parS* sequences are mainly clustered in the so-called *ori* domain comprising ca. 20% of the chromosome [7].

The role of the ParABS systems in accurate bacterial chromosome segregation is widely acknowledged but varies from essential, as exemplified by *Caulobacter crescentus* [8] or *Myxococcus xanthus* [9], to accessory, as in *Bacillus subtilis* [10–13], *Streptomyces coelicolor* [14], *Vibrio cholerae* [15,16] or *Pseudomonas aeruginosa* [17–19]. Apart from their well-established role in the segregation of newly replicated *ori* domains through DNA compaction [20–22], proper positioning of *ori* domains in the cell [19,23], Par proteins have also been shown to play a role in the control of DnaA activity and replication initiation [24,25] as well as in coordination of cell cycle and differentiation [26–28]. Chromosomal ParB homologs bind to *parS in vitro*, polymerize on DNA and bridge distant sequences

bioRxiv preprint doi: https://doi.org/10.1101/151340; this version posted June 20, 2017. The copyright holder for this preprint (which was not certified by peer review) is the author/funder, who has granted bioRxiv a license to display the preprint in perpetuity. It is made available under aCC-BY-NC-ND 4.0 International license.

[13,29–32]. Whole-genome analyses using chromatin immunoprecipitation (ChIP) have demonstrated spreading of ParB homologs around *parS* sites for up to 20 kb [5,26–29]. Despite the ParB spreading, a transcriptomic analysis in *B. subtilis* did not identify any significant changes in gene expression in a *spo0J* null mutant (Spo0J is a ParB homolog) relative to a WT strain [35]. Limited ParB-dependent transcriptional silencing in the proximity of *parS* sequences has been observed only for several genes in *V. cholerae* [34] and *S. pneumoniae* [36].

In *P. aeruginosa* a lack of ParA and/or ParB is not lethal but results in up to 1000-fold increased frequency of production of anucleate cells even during growth in optimal conditions [17,18,37]. Various *par* mutants exhibit longer division time, increase in cell size, altered colony morphology and are impaired in swarming and swimming motility [17,18]. Ten *parS* sites scattered in the chromosome of *P. aeruginosa* have been identified, but only four of them closest to *oriC* seem to be involved in chromosome segregation [33,38]. A transcriptomic analysis of *P. aeruginosa parA* and *parB* mutants has demonstrated changes in expression of hundreds of loci [39], including genes related to stress response but also many known and putative transcriptional regulators, suggesting a direct and/or indirect role of Par proteins in the regulation of gene expression. In test plasmids, ParB of *P. aeruginosa* was found to spread around *parS* and silence nearby promoters [37], but a comparison of the *parB* mutant and WT transcriptomes did not reveal any obvious changes in the expression of genes adjacent to chromosomal *parS* sequences [39]. However, a recent ChIP-seq analysis of ParB distribution on the *P. aeruginosa* chromosome has revealed, in addition to the region around the high affinity *parS1-4* sequences, also secondary ParB binding sites, apparently not related to known *parS* sites [33].

Similarly to the lack of ParB, also its excess in *P. aeruginosa* affects the cell cycle, as highlighted by slower growth rate, and causes cell elongation and defects in swarming and

bioRxiv preprint doi: https://doi.org/10.1101/151340; this version posted June 20, 2017. The copyright holder for this preprint (which was not certified by peer review) is the author/funder, who has granted bioRxiv a license to display the preprint in perpetuity. It is made available under aCC-BY-NC-ND 4.0 International license.

swimming. ParB excess manifests in nucleoid condensation and increased frequency of anucleate cells formation [17,37,40,41]. The toxicity of ParB overproduction is significantly diminished when ParB is impaired in its polymerization domain [40] whereas ParB variants defective in interactions with DNA, either due to the inability to form dimers or mutations in the DNA binding domain, demonstrate no toxicity [40,41]. This suggests that DNA binding and spreading of ParB protein is crucial for its biological function.

In this project we analysed changes in the transcriptome of *P. aeruginosa* cells with a slightly increased ParB level, not affecting growth rate and chromosome segregation, to define the primary targets of ParB.

Materials and methods

Bacterial strains and growth conditions

Bacterial strains used in this study are listed in Table 1. Cultures were grown in L broth [42] or on L agar (L broth solidified with 1.5% agar) at 37^{o}C. For selection of plasmids *Escherichia coli* media were supplemented with 150 μg ml^{-1} (liquid cultures) or 300 μg ml^{-1} (solid media) penicillin (Pn), 10 μg ml^{-1} chloramphenicol (Cm) or 50 μg ml^{-1} kanamycin (Km). Chloramphenicol at concentration 75 μg ml^{-1} (liquid cultures) and 150 μg ml^{-1} (solid media) was used to maintain plasmids in *P. aeruginosa*. 300 μg ml^{-1} carbenicillin (Cb) and 300 μg ml^{-1} rifampicin (Rif) was added to the solid medium for the selection of *P. aeruginosa* transconjugants in allele exchange procedure. To induce the expression from the *araBAD* promoter arabinose (Ara) was added to 0.02% to cultures of PAO1161 with pKGB8 (*araBAD*p) or pKGB9 (*araBAD*p-*parB*) and to 0.1% in PAO1161::*araBAD*p or PAO1161::*araBAD*p-*flag-parB* cultures. For MIC analysis of PAO1161 (pKGB8) and PAO1161 (pKGB9) and PAO1161 as a control, strains were grown in Mueller Hinton cation

bioRxiv preprint doi: https://doi.org/10.1101/151340; this version posted June 20, 2017. The copyright holder for this preprint (which was not certified by peer review) is the author/funder, who has granted bioRxiv a license to display the preprint in perpetuity. It is made available under aCC-BY-NC-ND 4.0 International license.

106 adjusted medium in the range of Ara concentrations (0, 0.02 and 0.2%) and in the presence of
107 a gradient of piperacillin, ticarcillin, ciprofloxacin, gentamicin, tobramycin or imipenem.

108 **Table 1 Bacterial strains used in this study.**

Strain	Description	Reference
Escherichia coli		
DH5α	F⁻ Φ80*lacZ*Δ*M15* Δ(*lacZYA-argF) U169 recA1 endA1 hsdR17* (r_{K-}, m_{K+}) *phoA supE44 λ thi-1 gyrA96 relA1*	[43]
S17-1	*pro* Δ*hsdR hsdM*⁺ *recA* Tp^R Sm^R ΩRP4-Tc::Mu Kn::Tn7	[44]
Pseudomonas aeruginosa		
PAO1161	PAO1161 Rif^R *leu*	[17]
PAO1161 $parB_{null}$	PAO1161 Rif^R *leu parB*1-18::*tetM*, Tc^R	[17]
PAO1161 $parS_{null}$	PAO1161 Rif^R with ten *parS* sequences mutated or deleted to impair ParB binding to these sequences	[38]
PAO1161::*araBAD*p	PAO1161 Rif^R with *araC araBAD*p T_{rrnB}[1] cassette integrated in intergenic region between *PA5412* and *PA5413* (at position 6091513 nt)	this study
PAO1161::*araBAD*p-*flag-parB*	PAO1161 Rif^R with *araC araBAD*p-*flag-parB* T_{rrnB} cassette integrated in intergenic region between *PA5412* and *PA5413* (at position 6091513 nt)	this study
PAO1161::*bexR*p-*lacZ*	PAO1161 Rif^R Cb^R with *bexR*p-*lacZ* cassette integrated in intergenic region between *PA5412* and *PA5413* (at position 6091513 nt)	this study

109 [1] T_{rrnB} transcriptional terminator of *E. coli rrnB* gene

110 **Transformation and conjugation procedures**

bioRxiv preprint doi: https://doi.org/10.1101/151340; this version posted June 20, 2017. The copyright holder for this preprint (which was not certified by peer review) is the author/funder, who has granted bioRxiv a license to display the preprint in perpetuity. It is made available under aCC-BY-NC-ND 4.0 International license.

Transformation of *E. coli* and *P. aeruginosa* was performed by standard procedures [43,45]. Conjugation between transformants of *E. coli* S17-1 and *P. aeruginosa* PAO1161 Rif^R was performed on solid media as described previously [37].

Plasmids and DNA manipulations

Plasmids used in this study are listed in Table 2. Plasmid manipulations were carried out by standard procedures [46]. Oligonucleotides used in this work are listed in Table S1. All new plasmid constructs were verified by sequencing at the Laboratory of DNA Sequencing and Oligonucleotide Synthesis, IBB PAS.

Table 2 Plasmids used in this study.

Plasmid	Description	Reference
pABB1.0	pBBRMCS1 derivative, BHR^1, $ori_{IncA/C}$, Cm^R	[47]
pABB28.2	pET28a with *his*-tag replaced by *flag*-tag, Km^R	this study
pAKE600	suicide vector, $oriV_{MB1}$, *sacB* gene, Pn^R	[48]
pBAD24	expression vector, $oriV_{MB1}$, *araC araBAD*p T_{rrnB} cassette, Pn^R	[49]
pCM132	BHR^1, dual replicon promoter-probe vector $oriV_{ColE1}$, $oriV_{RK2}$, $trfA_{RK2}$, $oriT_{RK2}$, promoter-less *lacZ*, Km^R	[50]
pET28a	expression vector, $oriV_{MB1}$, T7p, 6xHis-tag, Km^R	Novagen, Inc.
pKAB132	pPJB132 with deletion of EcoRI-BglII fragment, control vector, Cm^R, Km^R	this study
pKAB133	pPJB132 with *PA0011*p-*lacZ*	this study
pKAB134	pPJB132 with PA0011p$_{parS3mut}$-*lacZ*	this study
pKAB135	pPJB132 with *PA0013*p-*lacZ*	this study
pKAB136	pPJB132 with *PA0013*p$_{parS4mut}$-*lacZ*	this study
pKAB240	pBAD24 with NsiI restriction site between T_{rrnB} and *bla*p	this study
pKAB241	pKAB240 with *flag* tagged *P. aeruginosa parB* (*araBAD*p-*flag-parB*)	this study
pKAB242	pKAB240 with T_{rrnB}-*mcs*-*lacZ*(partial)-T_{T7}[2] cassette inserted as	this study

bioRxiv preprint doi: https://doi.org/10.1101/151340; this version posted June 20, 2017. The copyright holder for this preprint (which was not certified by peer review) is the author/funder, who has granted bioRxiv a license to display the preprint in perpetuity. It is made available under aCC-BY-NC-ND 4.0 International license.

	NsiI fragment	
pKAB243	pKAB242 with insertion of full-length *lacZ* and *mcs*, contains complete T_{rrnB}-*mcs*-*lacZ*-T_{T7} cassette (NsiI fragment)	this study
pKAB600	pAKE600 with *P. aeruginosa* genomic fragment (coordinates 6090756 - 6092192) with PstI at position 6091513 nt	this study
pKAB601	pKAB600 with *araC araBAD*p T_{rrnB} cassette	this study
pKAB602	pKAB600 with *araC araBAD*p-*flag*-*parB* T_{rrnB} cassette	this study
pKAB603	pKAB600 with deletion of EcoRI restriction site	this study
pKAB604	pKAB603 with T_{rrnB}-*mcs*-*lacZ*-T_{T7} cassette	this study
pKAB605	pKAB604 with *BexR*p cloned in the *mcs*, T_{rrnB}-*BexR*p-*lacZ*-T_{T7} cassette	this study
pKGB8	pABB1.0 with *araC araBAD*p, expression vector	this study
pKGB9	pKGB8 with *araBAD*p-$parB_{P.a.}$	this study
pKRP10	ori_{MB1}, contains Cm^R cassette, Pn^R	[51]
pMKB5.2	$oriV_{MB1}$, *cyaA*T18-$parB_{P.a}$ translational fusion, Pn^R	[48]
pPJB132	pCM132 with Cm^R cassette, Cm^R, Km^R	this study

[1] BHR, broad-host-range plasmid

[2] T_{T7}, T7 phage transcriptional terminator

Plasmid pKGB8 was constructed by ligation of Eco47III-PstI fragment from pBAD24 containing *araC araBAD*p with HincII and PstI digested pABB1.0. Subsequently, EcoRI-SacI fragment from pMKB5.2 containing *parB* ORF was cloned into pKGB8 to yield plasmid pKGB9.

pET28a (Novagen, Inc.) was modified to add *flag*-tag instead of *his*-tag to the coding sequences. Oligonucleotides #1 and #2 were combined, heated to 100°C for 5 minutes and left for annealing at room temperature. pET28a vector was digested using NcoI and NdeI and ligated with obtained synthetic DNA fragment to yield pABB28.2.

To facilitate transfer of the *araC-araBAD*p-T_{rrnB} cassette, an additional NsiI restriction site was introduced into pBAD24 downstream of T_{rrnB}. Two fragments amplified by PCR

bioRxiv preprint doi: https://doi.org/10.1101/151340; this version posted June 20, 2017. The copyright holder for this preprint (which was not certified by peer review) is the author/funder, who has granted bioRxiv a license to display the preprint in perpetuity. It is made available under aCC-BY-NC-ND 4.0 International license.

using pBAD24 as a template and primer pairs #3/#4 and #5/#6, respectively, were used as a template in the second round of PCR with primers #3 and #6 to obtain a 1160 bp product that replaced the HindIII-ScaI fragment in pBAD24 to yield pKAB240.

The *flag-parB* fusion was constructed using similar strategy. The *flag* sequence amplified from pABB28.2 using primers #7/#8 and *P. aeruginosa parB* gene amplified from PAO1161 genomic DNA using primers #9/#10 were combined and used as a template in overlap PCR with primers #7/#10. The obtained PCR fragment with *flag-parB* fusion was digested with EcoRI and SalI and ligated into pKAB240 to yield pKAB241.

To construct PAO1161::*araBAD*p and PAO1161::*araBAD*p-*flag-parB* strains, the suicide plasmids pKAB601 and pKAB602 were constructed. First, the intergenic region between *PA5412* and *PA5413* from PAO1161 chromosome was amplified in two parts with pairs of primers #11/#12 and #13/#14. Primers #12 and #13 introduced a PstI site. The obtained PCR fragments were digested either with MfeI and PstI or PstI and BamHI, respectively, and the mixture was ligated with EcoRI and BamHI digested pAKE600 [48] to yield pKAB600. The *araC-araBAD*p-T_{rrnB} cassette from pKAB240 and *araC-araBAD*p-*flag-parB*-T_{rrnB} cassette from pKAB241 were excised as NsiI fragments and ligated into PstI site of pKAB600 to yield pKAB601 and pKAB602, respectively. *E. coli* S17-1 strain was transformed with pKAB601 or pKAB602 and the transformants were used as donor strains in conjugation with PAO1161 Rif^R [18]. The cassettes were integrated in the defined region of PAO1161 using the allele exchange procedure [18] to obtain PAO1161::*araBAD*p and PAO1161::*araBAD*p-*flag-parB*.

pCM132 was modified by insertion of Cm^R cassette (SphI fragment from pKRP10 [51]) into SphI site, downstream of *lacZ*, to yield pPJB132. Putative promoter sequences preceding *PA0011* and *PA0013* were amplified on PAO1161 genomic DNA using primer pairs #15/#16 and #17/#18, respectively. The *PA0011*$p_{parS3mut}$ and *PA0013*$p_{parS4mut}$ fragments

bioRxiv preprint doi: https://doi.org/10.1101/151340; this version posted June 20, 2017. The copyright holder for this preprint (which was not certified by peer review) is the author/funder, who has granted bioRxiv a license to display the preprint in perpetuity. It is made available under aCC-BY-NC-ND 4.0 International license.

were amplified on PAO1161 *parS*$_{null}$ genomic DNA [38] as a template using the same primer pairs. PCR products were digested with EcoRI and BamHI and ligated between EcoRI and BglII sites into pPJB132 to yield plasmids pKAB133 (*PA0011*p-*lacZ*), pKAB134 (*PA0011*p$_{parS3mut}$-*lacZ*), pKAB135 (*PA0013*p-*lacZ*) and pKAB136 (*PA0013*p$_{parS4mut}$-*lacZ*). The empty control vector for β-galactosidase measurements (pKAB132) was obtained by digestion of pPJB132 with EcoRI and BglII, blunting by fill-in with Klenow fragment of DNA PolI and self-ligation.

To construct PAO1161 Rif^{R} strain with *bexR*p-*lacZ* cassette integrated in intergenic region between *PA5412* and *PA5413*, the suicide plasmid pKAB605 was constructed. First, the T$_{rrnb}$ with *mcs*, part of the *lacZ* gene and T$_{T7}$ was amplified using overlap PCR strategy. To this end, 2 fragments were amplified on pCM132 plasmid as a template using primer pairs #19/#20 and #21/#22, respectively, and the 3rd fragment was amplified on pET28a using primer pair #23/#24. The three fragments were mixed and used as a template in an overlap PCR with primers #19/#24. The obtained 787 bp product digested with NsiI replaced the *araC-araBAD*p-T$_{rrnB}$ in pKAB240 yielding plasmid pKAB242. *mcs-lacZ* was subsequently excised from pCM132 as EcoRI and BlpI fragment and ligated with EcoRI-BlpI digested pKAB242 to yield pKAB243, containing complete T$_{rrnB}$-*mcs-lacZ*-T$_{T7}$ cassette.

The single EcoRI restriction site in pKAB600 plasmid was removed by EcoRI digestion, filling in by Klenow fragment of DNA PolI and plasmid self-ligation to yield pKAB603. The T$_{rrnB}$-*mcs-lacZ*-T$_{T7}$ cassette excised from pKAB243 by NsiI digestion was ligated into PstI site of pKAB603 to yield pKAB604. The region preceding *bexR* (*PA2432*) gene was amplified on PAO1161 genomic DNA using primers #25/#26, digested with EcoRI and BamHI and ligated with EcoRI and BglII digested pKAB604 to yield plasmid pKAB605 carrying T$_{rrnB}$- *bexR*p-*lacZ*-T$_{T7}$ cassette flanked by sequences allowing integration in the intergenic region between *PA5412* and *PA5413*. *E. coli* S17-1 strain transformed with

bioRxiv preprint doi: https://doi.org/10.1101/151340; this version posted June 20, 2017. The copyright holder for this preprint (which was not certified by peer review) is the author/funder, who has granted bioRxiv a license to display the preprint in perpetuity. It is made available under aCC-BY-NC-ND 4.0 International license.

183 pKAB605 was used as donor in conjugation with PAO1161 Rif^R [18]. The suicide vector was
184 integrated in the defined region of PAO1161 (at position 6091513 nt) using homology
185 recombination [18] and the carbenicillin-resistant integrant (PAO1161::*bexR*p-*lacZ*) was used
186 as a recipient in a subsequent conjugation with S17-1 cells carrying pKGB8 or pKGB9
187 plasmids. Transconjugants were selected on L agar plates with carbenicillin, chloramphenicol
188 and 40 μg ml^{-1} X-gal to allow visualization of *bexR*p-*lacZ* induction immediately after the
189 introduction of plasmids.

190 **RNA isolation**

191 *P. aeruginosa* strains taken from -80^{o}C stocks were grown on L agar plates at 37^{o}C
192 and single colonies were used to inoculate three independent cultures (biological replicates).
193 After overnight growth, the cultures were diluted 1:100 into fresh L broth and grown to the
194 optical density 0.4- 0.6 at 600 nm (OD_{600}). RNA was isolated with RNeasy mini kit (Qiagen)
195 according to the manufacturer's protocol for bacterial cells from 2 ml of cultures mixed with 4
196 ml of RNAprotect Bacteria Reagent (Qiagen). Total RNA was digested with DNase (TURBO
197 DNA-free Kit, Ambion) to remove genomic DNA.

198 **Microarray analysis**

199 Microarray analysis was performed essentially as described before [39]. The raw
200 microarray data have been deposited at the NCBI Gene Expression Omnibus database at
201 accession number GSE95647 (release after publication acceptance). Gene expression data
202 were analysed using Partek Genomic Suite v6.6 (Partek Inc., St. Louis, MO). Raw data were
203 processed using GeneChip Robust Multiarray Averaging (GC RMA): background correction,
204 quantile normalization, log2 transformation and median polish summarization. Analysis of
205 variance (ANOVA) using REML (restricted maximum likelihood) was performed to identify
206 differentially expressed genes. Gene lists were created using a cut-off of p-value≤0.05, with a

bioRxiv preprint doi: https://doi.org/10.1101/151340; this version posted June 20, 2017. The copyright holder for this preprint (which was not certified by peer review) is the author/funder, who has granted bioRxiv a license to display the preprint in perpetuity. It is made available under aCC-BY-NC-ND 4.0 International license.

fold change (FC) higher than 2 or lower than -2. Clustering of the genes according to expression pattern changes was performed by K-means clustering [52] using MultiExperiment Viewer v4.9 [53]. The gene expression data for individual replicates were averaged, normalized to zero-mean and unit variance, and subjected to clustering into six clusters, using Pearson correlation as the distance metric and 500 as the maximum number of iterations.

RT-qPCR analysis

cDNA was synthesized with the TranScriba cDNA synthesis kit (A&A Biotechnology, Poland) using 1.5 μg of total RNA per reaction and random hexamer primers. RT-qPCR reactions were performed in a Roche LightCycler 480 using Hot FIREPol EvaGreen qPCR Mix Plus (Solis Biodyne). The reactions were performed with 0.15- 0.3 μl of cDNA in a total volume of 20 μl. Three technical replicates were used for each gene/primer combination. The primers used to amplify target and reference genes are listed in Table S1. Changes in the gene expression were calculated using the Pfaffl method [54] with normalization to the reference gene *nadB* (*PA0761*). RT-qPCR data represent mean for 3 biological replicates and 3 technical replicates. All RT-qPCR experiments were repeated twice and representative experiments are shown.

Western blotting

Cultures were grown on L broth to OD_{600} 0.4-0.6. Cells were harvested by centrifugation and stored at -20^{o}C. For each sample a small aliquot was used to estimate the number of c.f.u. ml^{-1} by plating appropriate dilution of the culture on L agar plates. Pellets were resuspended in 10 mM Tris-HCl (pH 8.0), 1 M NaCl, 0.1 mM EDTA, 5% glycerol. For each sample different volume of the buffer was used to compensate the initial differences in c.f.u. ml^{-1}. Samples were sonicated and aliquots of cleared extracts corresponding to 10^9 cells were separated by SDS-PAGE on 12% polyacrylamide gels. Additionally, His_6-ParB, purified

bioRxiv preprint doi: https://doi.org/10.1101/151340; this version posted June 20, 2017. The copyright holder for this preprint (which was not certified by peer review) is the author/funder, who has granted bioRxiv a license to display the preprint in perpetuity. It is made available under aCC-BY-NC-ND 4.0 International license.

as described [37], was loaded on each gel. Separated proteins were transferred onto nitrocellulose membranes. The blots were subjected to a two-step immunoreaction including application of rabbit polyclonal anti-ParB antibodies followed by incubation with goat anti-rabbit antibodies conjugated with alkaline phosphatase and were developed by addition of NBT/ BCIP mixture. Band intensity was estimated using ImageJ for at least 3 biological replicates.

Biofilm formation assay

Biofilm formation in static cultures was assayed as described previously with minor modifications [55]. Overnight cultures of *P. aeruginosa* strains in three biological replicates were diluted 1:100 in L broth with or without 0.02% arabinose. 75 μg ml^{-1} chloramphenicol was added to maintain the plasmids. 100 μl aliquots of each diluted culture were transferred into 9 wells of a 96-well flat-bottom polystyrene microplate (Greiner Bio-One). Sterile L broth was used as a negative control. The plate was incubated without shaking at 37°C until OD_{600} reached approximately 0.5. The optical density OD_{600} was measured using a plate reader (BioTek Synergy HT) and bacterial cells, which did not adhere to the surface, were gently removed by aspiration with a pipette. Wells were washed twice with 100 μl of PBS (15 mM KCl, 150 mM NaCl, 10 mM NaPi pH 7.4) and biofilm in each well was stained with 100 μl of 0.1% crystal violet solution. After 15 min incubation at room temperature, crystal violet solution was aspirated and wells were rinsed three times with distilled water and twice with 100 μl of PBS. Subsequently, 100 μl of 96% ethanol was added to each well and left for 10 min to dissolve the crystal violet. Well content was mixed by pipetting and OD_{590} was measured using a plate reader and 96% ethanol as a blank. Biofilm formation is presented as proportion OD_{590}/OD_{600}.

β-galactosidase activity assays

bioRxiv preprint doi: https://doi.org/10.1101/151340; this version posted June 20, 2017. The copyright holder for this preprint (which was not certified by peer review) is the author/funder, who has granted bioRxiv a license to display the preprint in perpetuity. It is made available under aCC-BY-NC-ND 4.0 International license.

β-galactosidase activity was measured as described before [42]. Extracts were prepared from cells grown to OD_{600} 0.4-0.6 in L broth with 75 μg ml^{-1} chloramphenicol, with or without 0.1% arabinose.

Results

Impact of *parB* overexpression on gene expression in *P. aeruginosa*

Our previous microarray analysis revealed altered expression of 1166 genes in ParB-deficient cells of *P. aeruginosa* relative to the wild type PAO1161 (WT) cells [39]. To complement this study, here we analysed the transcriptome of ParB -overproducing cells. To control the level of *parB* expression we constructed a pKGB8 expression vector based on the broad-host-range pBBR1MCS-1 [56], which contains the arabinose (Ara) inducible promoter *araBAD*p [49]. Analysis of the growth of PAO1161 (pKGB9 *araBAD*p-*parB*) and PAO1161 (pKGB8) cells in the presence of different concentrations of Ara revealed that induction by Ara ≤0.02% did not affect the growth (Fig 1A). A slight increase in the ParB level (≤2-fold) was observed even in non-induced cells of PAO1161 (pKGB9) relative to the cells containing the empty vector according to Western blot analysis (Fig 1B). Addition of 0.02% Ara to the medium resulted in a 5-fold increase in the ParB amount per cell in mid-log phase cultures of PAO1161 (pKGB9) in comparison to PAO1161 (pKGB8) (Fig 1B). Such ParB excess did not affect the frequency of anucleate cells formation, cell size, colony morphology or swimming and swarming motility (data not shown) but led to altered biofilm formation under specific conditions (Fig 1C, discussed below).

Fig 1. Effects of ParB excess in *P. aeruginosa*.

(**A**) Growth of *P. aeruginosa* PAO1161 (pKGB8 *araBAD*p) and PAO1161 (pKGB9 *araBAD*p-*parB*) strains in L broth with different arabinose concentrations. Data represent mean OD_{600}. (**B**) Western blot analysis of ParB levels in the tested strains. Each lane contains

bioRxiv preprint doi: https://doi.org/10.1101/151340; this version posted June 20, 2017. The copyright holder for this preprint (which was not certified by peer review) is the author/funder, who has granted bioRxiv a license to display the preprint in perpetuity. It is made available under aCC-BY-NC-ND 4.0 International license.

279 extract from 10^9 cells. Blots were subjected to immunodetection using primary anti-ParB
280 antibodies. Representative blot is shown. Signals on the blots were quantified. Data represent
281 mean ParB level ±SD relatively to the control strain PAO1161 (pKGB8). Purified His_6-ParB
282 was used to generate standard curves. M – molecular weight marker. **(C**) Biofilm formation in
283 the static cultures of PAO1161, PAO1161 (pKGB8) and PAO1161 (pKGB9). Strains were
284 grown without or with 0.02% arabinose until OD_{600} 0.5. Biofilm was stained with crystal
285 violet and assessed by measurement of OD_{590}. Data represent mean OD_{590}/OD_{600} ratio ±SD
286 from 3 biological replicates. * - *p*-value < 0.05 in two-sided Student's *t*-test assuming equal
287 variance.

288 To determine the impact of an increased ParB level on the transcriptome a microarray
289 analysis was performed on RNA isolated from PAO1161 (pKGB9 *araBAD*p-*parB*) cultures
290 grown under selection in L broth with 0.02% Ara (higher ParB overproduction, hereafter
291 referred to as ParB+++) or without Ara (mild ParB overproduction, hereafter called ParB+)
292 as well as from PAO1161 (pKGB8) cells grown under selection in L broth with 0.02% Ara
293 (empty vector control, hereafter EV) and PAO1161 cells grown in L broth without Ara (wild-
294 type control, hereafter WT). A principal component analysis of the microarray data revealed
295 that the biological replicates for WT and EV form 2 separate groups whereas the biological
296 replicates of ParB+ and ParB+++ form together a separate group, distinct from WT and EV
297 samples (data not shown).

298 Comparative transcriptome analysis of EV *vs* WT revealed 70 genes, four tRNA
299 genes, and four intergenic regions with an altered expression in response to the presence of
300 the vector [fold change (FC) <-2 or >2, *p*-value <0.05] (Fig 2A, Table S2). 175 genes and 1
301 intergenic region displayed statistically significant difference in expression between
302 ParB+++ and EV cells using the same criteria. 155 out of 175 genes displayed an altered
303 expression only in the response to the ParB abundance since they were not identified in the

bioRxiv preprint doi: https://doi.org/10.1101/151340; this version posted June 20, 2017. The copyright holder for this preprint (which was not certified by peer review) is the author/funder, who has granted bioRxiv a license to display the preprint in perpetuity. It is made available under aCC-BY-NC-ND 4.0 International license.

EV *vs* WT analysis. The expression of the remaining 20 genes and one intergenic region was affected by the presence of vector as well as ParB overproduction in ParB+++ cells (Fig 2B, Table S2). The comparative analysis of ParB+ and EV transcriptomes revealed altered expression of 157 genes. There was a major overlap between the transcriptomic changes in ParB+ and ParB+++ cells as 122 genes showed similar responses in the ParB+ and ParB+++ cells (Fig 2B, Table S2). This is not surprising as the transcription of *parB* (*PA5562*) itself was increased 4- and 12- fold in ParB+ and ParB+++ cells, respectively, in comparison to the EV cells.

Fig. 2. Transcriptome changes in response to ParB overproduction.

(**A**) Statistics of loci with significant expression change (FC<-2 or >2, *p*-value <0.05). RNA was isolated from PAO1161 cultures grown in L broth without Ara (WT), PAO1161 (pKGB8 *araBAD*p) cultures grown under selection in L broth with 0.02% Ara (empty vector control, EV), PAO1161 (pKGB9 *araBAD*p-*parB*) cultures grown under selection in L broth without Ara (mild ParB excess, ParB+) or with 0.02% Ara (higher ParB excess, ParB+++). (**B**) Venn diagram for sets of loci with significant expression change between EV *vs* WT, ParB+ *vs* EV and ParB+++ *vs* EV. (**C**) Classification of loci with altered expression according to PseudoCAP categories [57]. When a gene was assigned to multiple categories, one category was arbitrarily selected (Table S2). The PseudoCAP categories were grouped into six classes as marked. White and black bars correspond to the numbers of respectively, upregulated and downregulated genes in a particular category.

Interestingly, there was also a set of 35 genes with expression changed only in ParB+ cells relative to EV cells but not in ParB+++. Closer inspection of the expression changes of these genes revealed three subgroups (Fig S1A, Table S2): i/ 15 genes were also altered in ParB+++ transcriptome but with a slightly lower fold change (FC>1.6 or FC<-1.6, *p*-value

bioRxiv preprint doi: https://doi.org/10.1101/151340; this version posted June 20, 2017. The copyright holder for this preprint (which was not certified by peer review) is the author/funder, who has granted bioRxiv a license to display the preprint in perpetuity. It is made available under aCC-BY-NC-ND 4.0 International license.

328 <0.05) and were cut off from the common pool of ParB -affected genes using the criterion of
329 FC, ii/ 6 genes despite their high FC were eliminated in ParB+++ vs EV analysis because of
330 slightly higher variation of their expression in biological replicates (0.05< *p*-value <0.1), iii/
331 remaining 14 genes seemed to be not altered in ParB+++ transcriptome. Whereas ParB+++
332 and EV strains were grown under the same conditions (chloramphenicol and 0.02%
333 arabinose), ParB+ cells were not exposed to arabinose. To estimate the impact of inducer on
334 gene expression PAO1161 (pKGB8) was grown in medium with or without 0.02% Ara and
335 RT-qPCR analysis of eight loci from the group of 35 genes in question, representing all three
336 subgroups, was performed. The expression of only one gene, *PA2113* (from the bi-cistronic
337 operon *PA2113-2114*) was altered in response to Ara presence in the medium (Fig S1B).
338 *PA2113-2114* belong to the third subgroup in the expression pattern analysis (see above) but
339 also to a distinct set of 4 genes common for EV *vs* WT and ParB+ *vs* EV lists (Fig 2B, Table
340 S2), hence it is likely that these four genes appeared in our analysis due to the influence of
341 Ara on their expression. Presence of Ara had no influence on the expression of 7 out of 8
342 genes tested, which represent 14 genes due to the operon structures (Fig S1B), confirming that
343 majority of genes with the expression altered in ParB+ cells relative to EV cells was identified
344 due to their response to ParB excess.

345 The genes with altered expression were assigned to PseudoCAP categories [57]
346 divided arbitrarily into six classes as described previously [39]. The comparison of the EV
347 and WT transcriptomes revealed that the majority of affected genes belong to three groups:
348 Class II comprising genes encoding membrane proteins, proteins involved in transport of
349 small molecules, and protein secretion systems (18 genes), Class V comprising genes
350 involved in metabolic pathways (21 genes), and Class VI with 22 HUU genes (hypothetical,
351 unclassified, unknown) (Fig. 2C, Table S2). Similarly, most of the genes with altered
352 expression in ParB overproducing cells (ParB+++ and ParB+) relative to EV cells were

bioRxiv preprint doi: https://doi.org/10.1101/151340; this version posted June 20, 2017. The copyright holder for this preprint (which was not certified by peer review) is the author/funder, who has granted bioRxiv a license to display the preprint in perpetuity. It is made available under aCC-BY-NC-ND 4.0 International license.

353 assigned to the same three classes (II, V and VI). However, almost one third of the genes with
354 expression altered in response to ParB overproduction fall into Class I, mainly to PseudoCAP
355 categories RPTP (related to phage, transposon, plasmids) and SF (secreted factors: toxins,
356 enzymes, alginate). These data suggest that an increased ParB level leads to the activation of
357 stress response.

358 **Different expression patterns of genes affected by ParB excess**

359 To systematize the impact of the vector as well as the increased level of ParB on the
360 PAO1161 transcriptome a K-means clustering analysis was performed [52]. The two lists of
361 altered genes (ParB+ vs EV and ParB+++ vs EV) were combined yielding 211 unique loci
362 (Table S2). Expression data for replicates for each of these loci in the four strains/ growth
363 conditions (WT, EV, ParB+, ParB+++) were averaged, normalized to zero mean and unit
364 variance and grouped into six clusters based on the similarity of their expression patterns (Fig
365 3A and B).

366 **Fig 3. K-means clustering of microarray data.**

367 Expression data for replicates for each of 211 loci displaying altered expression in ParB
368 overproducing cells were averaged, normalized to zero mean and unit variance and grouped
369 into six clusters. (**A**) Expression profiles of individual genes grouped according to the results
370 of K-means clustering. Each horizontal line represents one gene. Red and blue denote that the
371 expression is respectively, above or below the mean expression of a gene across the data set.
372 (**B**) Expression profiles for genes in each cluster. Y-axis represents the difference between
373 expression of a particular gene in tested conditions and the mean expression of this gene in all
374 4 conditions presented as the number of standard deviations that a particular data point differs
375 from the mean. Thick black lines represent the cluster centres. The genes from each cluster
376 and their expression levels in different cells are listed in Table S3.

bioRxiv preprint doi: https://doi.org/10.1101/151340; this version posted June 20, 2017. The copyright holder for this preprint (which was not certified by peer review) is the author/funder, who has granted bioRxiv a license to display the preprint in perpetuity. It is made available under aCC-BY-NC-ND 4.0 International license.

Clusters 1 to 4 contain genes that are upregulated in ParB+ and/or ParB+++ cells relative to EV cells and clusters 5 and 6 the downregulated ones. A detailed description of the genes in each cluster as well as their mean expression levels in the four conditions are given in Table S3.

To validate the expression patterns obtained from the microarray analysis the transcript level for selected genes from each cluster in various samples was analysed using RT-qPCR. Importantly, for all tested 12 genes their relative levels of expression detected by RT-qPCR correlated nearly perfectly with the microarray data (Table 3).

Table 3 Validation of the microarray data by RT-qPCR.

		WT		EV	ParB+		ParB+++	
Cluster	**Gene ID**	**MA**	**qPCR**	**qPCR**	**MA**	**qPCR**	**MA**	**qPCR**
1	*PA0612*	0.66	0.76 ± 0.22	1 ± 0.06	6.54	5.62 ± 0.97	10.57	9.69 ± 3.3
1	*PA0985*	0.83	0.87 ± 0.16	1 ± 0.32	3.57	5.7 ± 1.67	5.02	7.1 ± 2.14
1	*PA4635*	0.60	0.48 ± 0.08	1 ± 0.12	2.95	1.42 ± 0.47	4.63	2.39 ± 1.12
1	*PA5562*	0.93	0.94 ± 0.21	1 ± 0.08	4.31	2.49 ± 0.43	12.06	17.3 ± 3.21
2	*PA2432*	0.62	0.57 ± 0.18	1 ± 0.29	8.36	5.13 ± 1.13	7.90	6.74 ± 0.1
2	*PA3661*	1.16	1.15 ± 0.45	1 ± 0.18	17.50	5.78 ± 2.23	23.34	8.39 ± 4.41
2	*PA5471*	0.24	0.28 ± 0.08	1 ± 0.25	2.24	2.01 ± 0.66	2.50	2.34 ± 0.34
3	*PA2008*	2.44	3.03 ± 1.06	1 ± 0.27	6.26	7.91 ± 1.36	3.81	3.91 ± 0.09
4	*PA4659*	1.73	0.97 ± 0.13	1 ± 0.13	1.83	2.23 ± 0.22	2.13	2.06 ± 0.1
5	*PA0996*	0.75	0.57 ± 0.01	1 ± 0.15	0.58	0.63 ± 0.22	0.31	0.33 ± 0.04
5	*PA1003*	0.87	0.73 ± 0.13	1 ± 0.24	0.72	0.58 ± 0.05	0.45	0.44 ± 0.04
6	*PA0011*	0.96	1.01 ± 0.2	1 ± 0.24	0.37	0.41 ± 0.03	0.20	0.24 ± 0.00

Relative transcript level of selected genes in replicates of *P. aeruginosa* cultures assessed by microarrays and RT-qPCR. WT - PAO1161 grown in L broth, EV - PAO1161 (pKGB8) grown in L broth with 0.02% Ara,

bioRxiv preprint doi: https://doi.org/10.1101/151340; this version posted June 20, 2017. The copyright holder for this preprint (which was not certified by peer review) is the author/funder, who has granted bioRxiv a license to display the preprint in perpetuity. It is made available under aCC-BY-NC-ND 4.0 International license.

ParB+ - PAO1161 (pKGB9) grown in L broth and ParB+++ - PAO1161 (pKGB9) grown in L broth with 0.02% Ara. Microarray (MA) data represent mean expression and RT-qPCR (qPCR) data represent mean ±SD from three biological replicates.

Genes upregulated in response to *parB* overexpression

Clusters 1 (64 genes and one intergenic region), 2 (48 genes), 3 (21 genes) and 4 (12 genes) contain loci upregulated in response to ParB overproduction. For eight of these loci an increased transcript level is also observed in EV cells relative to WT cells (Table S3, Table 4). Among these loci are *PA5471* gene encoding ArmZ, an inhibitor of MexZ which negatively regulates the *mexXY* operon encoding the multidrug efflux pump MexXY [58,59] and *pyeR* (*PA4354*) encoding a transcriptional regulator of biofilm formation [60]. Additionally, Cluster 1 contains the *arr* (*PA2818*) gene predicted to encode a phosphodiesterase whose substrate is cyclic di-guanosine monophosphate (c-di-GMP), a bacterial secondary messenger that regulates cell surface adhesiveness, virulence and biofilm formation [61].

The biofilm formation was checked in the cultures of PAO1161 (pKGB9 *araBAD*p-*parB*) in comparison to PAO1161 (pKGB8) during growth under static conditions. No difference was observed between the strains in the overnight cultures (data not shown). Notably, a significant increase in biofilm formation was observed in dividing cultures of PAO1161 (pKGB9 *araBAD*p-*parB*) relative to PAO1161 (pKGB8), which correlates with the altered expression of genes involved in regulation of biofilm formation and identified in our study. No effect of arabinose presence on biofilm formation was detected (Fig 1C). Transcriptomic analysis also implicated that ParB excess could alter the response to antibiotic presence. The MICs for six antibiotics from β-lactam, aminoglycoside and fluorochinolone groups (piperacillin, ticarcillin, imipenem, gentamicin, tobramycin and ciprofloxacin) were tested but no significant differences between PAO1161 (pKGB9) and control PAO1161(pKGB8) strains grown with and without arabinose were detected (data not shown).

bioRxiv preprint doi: https://doi.org/10.1101/151340; this version posted June 20, 2017. The copyright holder for this preprint (which was not certified by peer review) is the author/funder, who has granted bioRxiv a license to display the preprint in perpetuity. It is made available under aCC-BY-NC-ND 4.0 International license.

413 **Table 4 Selected genes whose expression was identified as ParB regulated.**

ID	Gene	Fold change			Cluster	Description
		EV *vs* WT	ParB+ *vs* EV	ParB+++ *vs* EV		
Genes induced by the presence of vector as well as ParB excess						
PA0805		3,3		2,2	1	hypothetical protein
PA1394		2,1	2,0	2,7	1	hypothetical protein
PA2288		2,2	2,3	4,2	1	hypothetical protein
PA4354	*pyeR*	3,2		2,3	1	ArsR-family transcriptional repressor
PA4826		2,6		2,5	1	hypothetical protein
PA5470		7,1	2,3	3,0	1	probable peptide chain release factor
PA5471	*armZ*	4,1	2,2	2,5	2	MexZ anti-repressor
Selected phage-related genes and pyocins						
PA0610	*prtN*		2,8	5,4	1	transcriptional regulator PrtN
PA0612	*ptrB*		6,5	10,6	1	repressor PtrB
PA0907	*alpA*		3,4	4,3		transcriptional regulator
PA0985	*pyoS5*		3,6	5,0	1	pyocin S5
PA1150	*pys2*		2,9	4,1	1	pyocin S2
PA3866			2,6	4,1	1	Pyocin S4
Genes related to type VI export						
PA0083	*hsiB1*		2,0	2,3	2	sheath protein, Hcp secretion island I
PA0084	*tssC1*		2,2	2,1	2	TssC1, Hcp secretion island I
PA0085	*hcp1*		2,3	2,2	2	Hcp1, Type VI secretion system effector
PA0087	*tssE1*			2,2	2	component of Hcp secretion island I
PA0089	*tssG1*		2,2	2,5	2	component of Hcp secretion island I
PA0090	*clpV1*		2,7	2,7	2	putative ATPase, Hcp secretion island I
PA0091	*vgrG1a*		2,6	2,8	2	component of Hcp secretion island I
PA0095	*vgrG1b*		2,1		4	secreted protein of unknown function
PA1844	*tse1*			2,0	1	toxin
PA1845	*tsi1*		2,2	2,6	2	immune protein
Genes regulated by BexR						
PA2432	*bexR*		8,4	7,9	2	bistable expression regulator
PA2433			3,4	4,5	1	hypothetical protein
PA1202			6,9	5,8	2	probable hydrolase
PA1203			3,3	3,2	2	hypothetical protein
PA1204			2,3	2,2	2	NAD(P)H quinone oxidoreductase
PA1205			2,5	2,3	2	conserved hypothetical protein
PA2698			2,1	2,1	2	probable hydrolase
PA1337	*ansB*			-2,0	6	glutaminase-asparaginase
PA1338	*ggt*			-2,5	6	gamma-glutamyltranspeptidase precursor
PA1340	*aatM*			-2,8	6	putative amino acid transporter
PA1341	*aatQ*			-3,1	6	putative amino acid transporter
Genes involved in PQS synthesis						
PA0996	*pqsA*			-3,2	5	PqsA, probable coenzyme A ligase
PA0997	*pqsB*			-3,5	5	PqsB, probable beta-keto-acyl-acyl-carrier protein synthase
PA0998	*pqsC*		-2,0	-3,5	5	PqsC, probable beta-keto-acyl-acyl-carrier protein synthase
PA0999	*pqsD*		-2,1	-3,8	5	3-oxoacyl-[acyl-carrier-protein] synthase III

bioRxiv preprint doi: https://doi.org/10.1101/151340; this version posted June 20, 2017. The copyright holder for this preprint (which was not certified by peer review) is the author/funder, who has granted bioRxiv a license to display the preprint in perpetuity. It is made available under aCC-BY-NC-ND 4.0 International license.

PA1000	*pqsE*	-2,4	-3,7	5	quinolone signal response protein
PA1001	*phnA*	-2,5	-4,6	5	anthranilate synthase component I
PA1002	*phnB*		-3,1	5	anthranilate synthase component II
PA1003	*mvfR*		-2,2	5	transcriptional regulator MvfR
Pyochelin and pyoverdine biosynthesis genes					
PA4220		-2,0		5	hypothetical protein
PA4221	*fptA*	-2,6		5	Fe(III)-pyochelin outer membrane receptor precursor
PA4224	*pchG*	-2,6	-2,5	6	pyochelin biosynthetic protein PchG
PA4225	*pchF*	-2,4	-2,9	6	pyochelin synthetase
PA4228	*pchD*	-2,9	-2,3	5	pyochelin biosynthesis protein PchD
PA4229	*pchC*	-2,2		5	pyochelin biosynthetic protein PchC
PA4230	*pchB*	-2,4	-2,1	6	salicylate biosynthesis protein PchB
PA4231	*pchA*	-2,5	-2,3	5	salicylate biosynthesis isochorismate synthase
PA2384		-3,0		6	transcriptional regulator
PA2403		-3,1		6	hypothetical protein
PA2406		-2,7	-3,2	6	hypothetical protein
PA2409		-3,0	-2,8	6	probable permease of ABC transporter
PA2410		-3,0	-3,2	6	hypothetical protein
PA2411		-2,2		5	probable thioesterase
Transcriptional regulators					
PA0515		3,1	3,0	4	probable transcriptional regulator
PA1196		3,7	3,5	2	probable transcriptional regulator
PA2583			2,3	1	sensor/response regulator hybrid
PA4659			2,1	4	probable transcriptional regulator
PA4896		-2,1		5	probable sigma-70 factor, ECF subfamily
Genes adjacent to *parS1-4*					
PA0004	*gyrB*		-2,0	6	DNA gyrase subunit B
PA0005	*lptA*		-2,1	6	lysophosphatidic acid acyltransferase, LptA
PA0006			-2,1	6	conserved hypothetical protein
PA0008	*glyS*		-3,1	6	glycyl-tRNA synthetase beta chain
PA0009	*glyQ*		-2,5	6	glycyl-tRNA synthetase alpha chain
PA0011	*htrB1*	-2,7	-4,9	6	2-OH-lauroyltransferase
PA0012		-2,6	-3,7	6	hypothetical protein
PA0013		-3,4	-3,5	6	conserved hypothetical protein
Genes adjacent to *parS6*					
PA0492		-6,7	-2,8	6	conserved hypothetical protein
PA0493		-4,3	-2,4	6	probable biotin-requiring enzyme
PA0494		-3,0	-2,2	6	probable acyl-CoA carboxylase subunit
PA0495		-3,6	-2,1	6	hypothetical protein

A remarkable feature of clusters 1 and 2, comprising the majority of ParB -upregulated genes (Table S3), is a high proportion of phage-related genes (*PA0610*, *PA0612-0641*, *PA0643-0648*, *PA0717*, *PA0718*, *PA0907*, *PA0909-0911*) as well as pyocin-encoding genes (*PA0985*, *PA1150*, *PA3866*). Induction of bacteriophage genes and pyocin production in *P.*

bioRxiv preprint doi: https://doi.org/10.1101/151340; this version posted June 20, 2017. The copyright holder for this preprint (which was not certified by peer review) is the author/funder, who has granted bioRxiv a license to display the preprint in perpetuity. It is made available under aCC-BY-NC-ND 4.0 International license.

419 *aeruginosa* have been shown to be a hallmark of the SOS response [62], suggesting that *parB*
420 overexpression induces a DNA damage signal. In this bacterium SOS response is coordinated
421 not only by LexA (*PA3007*), but also by two structurally related repressors, PrtR (*PA0611*)
422 and AlpR (*PA0906*) [62,63]. Significantly, expression of none of these genes is affected by
423 ParB excess. PrtR is an inhibitor of *prtN* (*PA0610*), a transcriptional activator of pyocin
424 synthesis genes [64]. *prtN* is induced 5.4-fold in ParB+++ cells suggesting a relief of the
425 PrtR-mediated repression in these cells. Similarly, genes controlled by AlpR (*PA0907*,
426 *PA0909-PA0911*) are induced in response to ParB overproduction. Further studies are
427 required to determine the effect on the expression of the PrtR- and AlpR- regulated genes
428 apparently without a change in the amounts of transcript level of these two repressors.

429 The ParB excess also induces genes encoding components of the Hcp secretion island
430 HSI-1 [65] (*PA0083-0085, PA0087, PA0089-0091*) and the toxin/immunity proteins Tse1
431 (*PA1844)* and Tsi1 (*PA1845*). The HSI-1 together with two other secretion islands participate
432 in *P. aeruginosa* virulence, inter- and intraspecies antagonism, biofilm formation, and stress
433 sensing [66].

434 Overexpression of *parB* also results in an 8-fold increase in the expression of the
435 transcriptional regulatory gene *PA2432* encoding a bistable response regulator BexR [67]. Six
436 genes, *PA1202, PA1203, PA1204, PA1205, PA2433* and *PA2698,* previously identified as
437 upregulated in response to BexR overproduction [67], are also upregulated in ParB-
438 overproducing strains. Similarly, five genes downregulated in response to BexR
439 overproduction, *PA0998, PA1337, PA1338, PA1340* and *PA1341*, are also downregulated in
440 the analysed ParB -overproducing cells (Table 4).

441 The expression of *bexR* gene is known to be bistable, meaning that this gene switches
442 between OFF and ON states in cells of a genetically identical bacterial population [67]. The

bioRxiv preprint doi: https://doi.org/10.1101/151340; this version posted June 20, 2017. The copyright holder for this preprint (which was not certified by peer review) is the author/funder, who has granted bioRxiv a license to display the preprint in perpetuity. It is made available under aCC-BY-NC-ND 4.0 International license.

443 microarray analysis was performed on three independent biological isolates of PAO1161
444 (pKGB9 *araBAD*p-*parB*) and all demonstrated a strong induction of *bexR* (*PA2432*)
445 expression (*p*-value 3E-06) strongly suggesting that ParB excess modulates the BexR regulon
446 through induction of *bexR* expression. To monitor the effect of ParB excess on promoter of
447 *bexR* the strain PAO1161::*bexR*p-*lacZ* was constructed with the promoter-reporter cassette
448 inserted in a non-coding region of the genome. A single colony (white on L agar with X-gal)
449 was inoculated and the cells were used as the recipients in conjugation with either S17-1
450 (pKGB8) or S17-1 (pKGB9 *araBAD*p-*parB*). Conjugants were plated on selective medium
451 containing X-gal to visualize the expression of *bexR*p-*lacZ* transcriptional fusion. Conjugants
452 PAO1161::*bexR*p-*lacZ* (pKGB8) formed typical white/transparent colonies with a very low
453 frequency of blue ones (less than 0.1%) whereas majority of PAO1161::*bexR*p-*lacZ* (pKGB9)
454 conjugants formed blue colonies (Fig 4), confirming that ParB induces *bexR*p expression.

455 **Fig 4. ParB excess induces the expression of chromosomal *bexR*p-*lacZ* transcriptional**
456 **fusion.**

457 PAO1161::*bexR*p-*lacZ* strain contains *bexR*p-*lacZ* transcriptional fusion inserted in the
458 intergenic region of PAO1161 genome. White colony from L agar with X-gal was inoculated
459 and used as a recipient in conjugation with either S17-1 (pKGB8) or S17-1 (pKGB9
460 *araBAD*p-*parB*) donor cells. Conjugants were grown on selective L agar plates supplemented
461 with X-gal. The photographs show representative plates of PAO1161::*bexR*p-*lacZ* with both
462 plasmids.

463 Clusters 3 and 4 group 33 genes with mRNA level reduced in response to plasmid/
464 chloramphenicol/ arabinose (EV) but then increased by ParB excess. Twelve of the 33 genes
465 in this group belong to the PseudoCAP category carbon compounds catabolism (CCC) and
466 eight genes to the amino acid biosynthesis and metabolism (AABM) category (Table S3). The

bioRxiv preprint doi: https://doi.org/10.1101/151340; this version posted June 20, 2017. The copyright holder for this preprint (which was not certified by peer review) is the author/funder, who has granted bioRxiv a license to display the preprint in perpetuity. It is made available under aCC-BY-NC-ND 4.0 International license.

467 altered expression of genes from these categories suggests that ParB overproduction may
468 interfere with primary metabolism as an adaptive measure. Interestingly, three out of four
469 putative arabinose-dependent genes have also been classified into cluster 4. Additionally,
470 cluster 4 contains two putative transcriptional regulators: *PA0515*, which is a part of the *nir*
471 operon (denitrification operon), and *PA4659* with unknown function.

472 **Genes downregulated in response to *parB* overexpression**

473 Clusters 5 (31 genes) and 6 (34 genes) contain genes downregulated in response to
474 ParB overproduction but differ from each other by a moderate induction in EV cells seen in
475 Cluster 5. This cluster contains all genes from two operons, *pqsABCDE* (*PA0996-1000*) and
476 *phnAB* (*PA1001* and *PA1002*), involved in the production of *Pseudomonas* quinolone quorum
477 sensing signal (PQS) [68,69]. Interestingly, the same cluster contains *PA1003* (*mvfR/pqsR*)
478 which encodes a positive regulator of the both operons [70,71], suggesting that the
479 downregulation of the *pqs* and *phn* operons is a direct result of lower *mvfR* expression.
480 Interestingly, MvfR also acts as a negative regulator of type VI secretion system HSI-1 [66],
481 components of which are upregulated in response to ParB excess (Table 4 and see above).

482 Five genes (*PA4220*, *PA4221*, *PA4228*, *PA4229*, *PA4231*) from Cluster 5 and three
483 genes (*PA4224*, *PA4225*, *PA4230*) from Cluster 6 are involved in the biosynthesis and
484 transport of a siderophore, pyochelin. Pyochelin synthesis in *P. aeruginosa* cells is positively
485 regulated by the transcriptional regulator PA2384 [72], which is downregulated in ParB+
486 cells. Interestingly, biosynthesis of another siderophore, pyoverdine, also seems to be
487 negatively affected by ParB excess as the genes *PA2403*, *PA2406*, *PA2409* and *PA2410*
488 (Cluster 6) from the pyoverdine biosynthesis operon are significantly downregulated in ParB-
489 overproducing cells (Table 4).

490 **Analysis of ParB-related transcriptional silencing around *parS* sites**

bioRxiv preprint doi: https://doi.org/10.1101/151340; this version posted June 20, 2017. The copyright holder for this preprint (which was not certified by peer review) is the author/funder, who has granted bioRxiv a license to display the preprint in perpetuity. It is made available under aCC-BY-NC-ND 4.0 International license.

Analysis of the microarray data revealed that ParB overproduction reduces the expression of a number of genes in close proximity of *parS1-4* (Table 4). Closer inspection of the expression changes in this region revealed that genes *PA0003-PA0015*, with the exception of *PA0007*, *tag* (*PA0010*) and *PA0014*, show a significant (30%-80%, *p*-value <0.05), ParB dose-dependent downregulation (Fig 5A). RT-qPCR analysis revealed that in fact all genes from *PA0004* to *PA0014* are subject to significant downregulation (Fig 5B), suggesting that ParB bound to *parS1-4* negatively influences the expression of adjacent genes. To verify this hypothesis we analysed the expression of these genes in the $parB_{null}$ mutant, which does not produce ParB [18], and in the $parS_{null}$ mutant in which the *parS1-4* sequences had been mutated, so the ParB binding to these sequences was impaired [38]. In the both mutants only genes from *PA0010* to *PA0015* displayed significantly increased expression (Fig 5C) indicating that at its native level ParB acts as a major negative regulator of genes adjacent to intergenic *parS3* and *parS4* but not for the genes adjacent to intragenic *parS1* and *parS2*. Regulation of the expression of genes in *parS1-parS4* region seems to be a direct consequence of ParB binding to *parS1-parS4* as ParB overproduction in $parS_{null}$ cells did not lower the expression of *dnaA–trkA* (*PA0001-PA0016*) genes relatively to the control $parS_{null}$ cells carrying empty vector (Fig 5D, also see below).

Fig 5. Influence of ParB on gene expression in the *parS1-4* region.

(**A**) Mean level of expression of *dnaA-def* (*PA0001-PA0019*) genes in ParB+ and ParB+++ cells relative to EV as revealed by microarray analysis. Filled markers indicate statistically different expression relative to EV (*p*-value < 0.05 in ANOVA test). Arrangement of the genes in the chromosome is shown below. Operons (according to the DOOR 2.0 database [73]) are marked in grey. (**B**) Expression of *PA0001-PA0016* **(***dnaA–trkA*) genes in ParB+ and ParB+++ cells relative to EV cells. (**C**) RT-qPCR analysis of expression of *dnaA–trkA* genes in $parB_{null}$ and $parS_{null}$ strains relative to WT cells. Cells were grown in L broth. (**D**) RT-

bioRxiv preprint doi: https://doi.org/10.1101/151340; this version posted June 20, 2017. The copyright holder for this preprint (which was not certified by peer review) is the author/funder, who has granted bioRxiv a license to display the preprint in perpetuity. It is made available under aCC-BY-NC-ND 4.0 International license.

qPCR analysis of expression of *dnaA–trkA* genes in $parS_{null}$ (pKGB9 *araBADp-parB*) and $parS_{null}$ (pKGB8 *araBAD*p) relative to EV [PAO1161 (pKGB8 *araBAD*p)]. Cells were grown in L broth supplemented with chloramphenicol and 0.02% arabinose. RT-qPCR data represent mean ±SD from three biological replicates. Filled symbols indicate significantly different expression (*p*-value <0.05 in two-sided Student's *t*-test assuming equal variance) relative to the control cells labelled as blue squares. The differences in expression of genes in $parS_{null}$ (pKGB9) strain relative to $parS_{null}$ (pKGB8) strain are not statistically significant.

A similar inspection of the expression changes in proximity (±10 adjacent genes) of the remaining six *parS* sequences [38] revealed that overproduction of ParB lowers the expression of genes adjacent to *parS6* (Fig 6A, *PA0492-PA0496*) but not to the other *parS* sequences (data not shown). These results were confirmed by RT-qPCR (data not shown). However, the expression of *PA0492*, *PA0493* and *PA0494* as assayed by RT-qPCR was not significantly changed in $parB_{null}$ or $parS_{null}$ cells in comparison with the WT strain (Fig 6B), indicating that at its native abundance ParB is not a major effector of genes in this region.

Fig 6. Influence of ParB level on expression of genes adjacent to *parS6*.

(**A**) Mean level of expression of *PA0488–PA0498* genes in ParB+ and ParB+++ cells relative to EV cells (microarray data). Filled markers indicate statistically different expression relative to EV (*p*-value < 0.05 in ANOVA test). Operons (according to the DOOR 2.0 database [73]) are labelled with different shades of grey. (**B**) RT-qPCR analysis of expression of *PA0492*, *PA0493* and *PA0494* genes in $parB_{null}$ and $parS_{null}$ strains relative to WT cells. Data represent mean ±SD from three biological replicates. The differences between strains / conditions are not statistically significant (*p*-value > 0.05 in two-sided Student's *t*-test assuming equal variance).

bioRxiv preprint doi: https://doi.org/10.1101/151340; this version posted June 20, 2017. The copyright holder for this preprint (which was not certified by peer review) is the author/funder, who has granted bioRxiv a license to display the preprint in perpetuity. It is made available under aCC-BY-NC-ND 4.0 International license.

Regulation of *PA0011* and *PA0013* promoters by ParB interactions with *parS3* and *parS4* sequences

To further confirm that ParB binding to *parS3* and *parS4* affects the expression of adjacent genes the intergenic regions preceding *PA0011* and *PA0013* and their respective variants carrying mutated *parS3* and *parS4* (Fig 7A) [38] were cloned upstream of a promoter-less *lacZ* cassette in pPJB132, a derivative of pCM132 [50]. To produce an excess of ParB from the chromosome strain PAO1161::*araBAD*p-*flag-parB* was constructed with the expression cassette inserted in a non-coding region of the genome (Table 1). Growth of the PAO1161::*araBAD*p-*flag-parB* cells in a medium containing 0.1% arabinose results in the overproduction of Flag-ParB to a level that is not toxic for the cells (data not shown). All four pPJB132 derivatives were introduced into PAO1161::*araBAD*p-*flag-parB* as well as into control strain PAO1161::*araBAD*p with the empty expression cassette inserted in the same genomic position.

Analysis of the β-galactosidase activity in the transformants of the control strain revealed no effect of 0.1% arabinose on the promoters tested (Fig 7B). The nucleotide substitutions in *parS3* modifications (Fig 7A) did not affect the *PA0011*p activity (Fig 7B). Surprisingly, replacing *parS4* by a NcoI restriction site (deletion of 10 bp) resulted in a minor increase of the promoter strength in the *PA0013*p$_{parS4\text{mut}}$-*lacZ* fusion (Fig 7B). DNA sequence analysis of promoters' regions does not give a clear explanation of such effect (Fig 7A). The β-galactosidase activities detected in transformants of PAO1161::*araBAD*p-*flag-parB* were similar to those in the corresponding control strain and when the strains were grown without arabinose. However, upon induction of *flag-parB* expression with 0.1% arabinose a reduction of β-galactosidase activity was observed in PAO1161::*araBAD*p-*flag-parB* transformants carrying plasmids with the *PA0011*p-*lacZ* and *PA0013*p-*lacZ* transcriptional fusions but not plasmids with the *PA0011*p$_{parS3\text{mut}}$-*lacZ* or *PA0013*p$_{parS4\text{mut}}$-*lacZ* transcriptional fusions (Fig

bioRxiv preprint doi: https://doi.org/10.1101/151340; this version posted June 20, 2017. The copyright holder for this preprint (which was not certified by peer review) is the author/funder, who has granted bioRxiv a license to display the preprint in perpetuity. It is made available under aCC-BY-NC-ND 4.0 International license.

564 7C). These data confirmed that ParB negatively regulates expression of these two promoters
565 *in vivo* through interactions with *parS* sites.

566 **Fig 7. Influence of ParB on the activities of *PA0011* and *PA0013* promoters.**

567 (**A**) DNA sequences preceding *PA0011* (*PA0011*p) and *PA0013* (*PA0013*p) and their mutated
568 versions, *PA0011*p$_{parS3mut}$ and *PA0013*p$_{parS4mut}$, cloned upstream of promoter-less *lacZ* cassette
569 in pPJB132 are presented. Putative promoters' motifs, RBS sequences and start codons are
570 indicated. Promoter -35 and -10 boxes were predicted using BPROM [74]. β-galactosidase
571 activity was measured in extracts from PAO1161::*araBAD*p (control strain) (**B**) and
572 PAO1161::*araBAD*p-*flag-parB* (ParB-overproducing strain) (**C**) cells carrying pPJB132
573 derivatives as indicated. Data represent mean activity from at least three cultures ±SD. * - *p*-
574 value < 0.05 in two-sided Student's *t*-test assuming equal variance.

575 **Discussion**

576 In *P. aeruginosa*, partitioning protein ParB plays a non-essential but important role in
577 segregation of chromosomes. Its binding to at least one of the four *parS* sequences in the
578 *parS1-4* cluster, closest to *oriC,* is necessary and sufficient for accurate segregation [33,38].
579 The role of the remaining six *parS* sequences (four in the *ori* domain and two, *parS7* and
580 *parS8*, close to the terminus domain [38]) is not fully understood. Ten similarly distributed
581 *parS* sequences in *B. subtilis* have been shown to participate in SMC recruitment,
582 condensation and juxtapositioning of chromosome arms [75]. Several reports have indicated
583 that partitioning proteins may also modulate transcription of certain genes [34,36] but *P.*
584 *aeruginosa* seems to be unique, as inactivation of *parA* or *parB* leads to large-scale changes
585 of its transcriptome [39]. A lack or an excess of ParB protein is manifested by similar
586 phenotypic changes, including erratic chromosome segregation, increased rate of formation of
587 anucleate cells, cell elongation, disturbed division and defects in swarming and swimming

bioRxiv preprint doi: https://doi.org/10.1101/151340; this version posted June 20, 2017. The copyright holder for this preprint (which was not certified by peer review) is the author/funder, who has granted bioRxiv a license to display the preprint in perpetuity. It is made available under aCC-BY-NC-ND 4.0 International license.

588 [17,18,37]. To find out how such multiple effects arise, a microarray-based transcriptomic
589 analysis was performed of PAO1161 derivatives in which ParB level was increased either 2-
590 or 5- fold in comparison with the strain carrying empty vector. Since after binding to a
591 specific *parS* sequence ParB has the ability to spread on the adjacent DNA, we mainly
592 focused on expression of genes in the vicinity of *parS* sequences.

593 At tested ParB concentrations its binding to *parS* sites has no pronounced effect on
594 expression of genes around them with the exception of genes located in proximity of *parS1-4*
595 and *parS6*. Microarray and RT-qPCR data show convincingly that all the genes adjacent to
596 *parS1-4* (*PA0003* to *PA0015*) are downregulated in the presence of ParB excess (Fig 3A and
597 B). The interference of ParB with the expression of a vital replication operon (*dnaA-dnaN-*
598 *recF-gyrB*), likely caused by ParB binding to *parS1*/*parS2* sites within the *recF* gene, may
599 underlie the defects in cell division caused by a ParB excess larger than studied here. In
600 contrast, in cells lacking a functional ParB protein or carrying mutated *parS1-4* sequences
601 unable to bind ParB, RT-qPCR analysis revealed only upregulation of *PA0010-PA0015* genes,
602 located in proximity of the intergenic *parS3* and *parS4*. Linking the regions preceding
603 *PA0011* and *PA0013* to the promoter-less *lacZ* cassette confirmed the presence of functional
604 promoters in the cloned fragments. Both promoters were repressed by ParB excess provided
605 functional *parS3* and *parS4* were present, which confirmed that ParB binding directly affects
606 transcription in this region.

607 The product of *PA0011*, the 2-OH-lauroyltransferase HtrB1 is involved in lipid A
608 biosynthesis important for integrity of the outer membrane and cell envelope [76–78]. *htrB1*
609 expression is induced by sub-inhibitory concentrations of different antibiotics [78] or growth
610 at low temperature [77]. Inactivation of *htrB1* leads to pleiotropic effects, manifested by
611 increased susceptibility to surfactants and antibiotics, impaired swarming motility, growth
612 defects and induction of type III secretion system. Some of these effects are also observed

bioRxiv preprint doi: https://doi.org/10.1101/151340; this version posted June 20, 2017. The copyright holder for this preprint (which was not certified by peer review) is the author/funder, who has granted bioRxiv a license to display the preprint in perpetuity. It is made available under aCC-BY-NC-ND 4.0 International license.

613 under ParB excess. Conversely, expression of another HtrB homolog (*PA3242*) is
614 significantly reduced in *parB*$_{null}$ mutant [39]. Since inactivation of either of the *htrB* genes in
615 *P. aeruginosa* PAO1 leads to motility defects [77,79], this could explain the impaired motility
616 seen both when ParB is missing and when it is present in excess. Notably, also other genes
617 adjacent to *parS3* and *parS4* encode proteins with putative roles in response to cellular stress.
618 *tag* (*PA0010*) encodes a putative 3-methyladenine glycosidase I [80]. *PA0012* encodes a
619 protein with a predicted PilZ domain, which could bind cyclic di-GMP, an important
620 signalling molecule in *P. aeruginosa* [81,82]. Further studies are needed to characterize the
621 biological functions of all the genes adjacent to *parS3* and *parS4* and the role of ParB in their
622 regulation.

623 Apart from the genes in proximity to *parS3/-parS4*, also those close to *parS6* showed a
624 reduced expression in response to ParB excess, however, their expression was not altered in
625 *parB*$_{null}$ and *parS*$_{null}$ strains, suggesting that here the ParB involvement is a part of a more
626 complex regulatory circuit. No changes were observed in the transcription of genes adjacent
627 to *parS5* and *parS7-parS10* upon ParB excess. Indeed, a recent ChIP-seq analysis did not
628 indicate binding of ParB to these sequences *in vivo* in cells grown in minimal medium [33],
629 but instead showed the presence of nine additional ParB-bound sites. However, none of the
630 genes adjacent to those regions changed expression in response to ParB excess in cells grown
631 in conditions tested here (data not shown). It is likely that the interaction of ParB with such
632 secondary ParB binding sites, which is not required for chromosome segregation, may
633 strongly depend on experimental conditions. It would be therefore interesting to compare
634 ParB ChIP data obtained for cells grown in minimal vs. rich medium.

635 A comparison of the transcriptional changes in *parB* -deficient cells and cells
636 expressing ParB excess identified 87 genes found in both studies (Table S4) [39]. Expression
637 of 83 genes similarly responded to either lack or abundance of ParB. Majority of them seem

bioRxiv preprint doi: https://doi.org/10.1101/151340; this version posted June 20, 2017. The copyright holder for this preprint (which was not certified by peer review) is the author/funder, who has granted bioRxiv a license to display the preprint in perpetuity. It is made available under aCC-BY-NC-ND 4.0 International license.

638 to be involved in the stress adaptation. Only *PA0293*, *PA1894*, *PA2113* and *PA2792* showed
639 opposite trends of the response. These four genes are downregulated in *parB* -deficient cells
640 and upregulated in response to ParB excess, hence it is unlikely that, akin to genes in the
641 proximity of *parS3* and *parS4*, ParB directly affects their expression.

642 Our data indicate that ParB excess downregulates two operons *pqsABCDE* and *phnAB*
643 involved in quinolone quorum sensing signalling [68,69], probably indirectly by repressing
644 *PA1003* (*mvfR/pqsR*) coding for a transcriptional activator of the both operons [70,71].
645 Additionally, the ParB excess interferes with expression of key virulence determinants, two
646 pathways involved in the production of the siderophores pyochelin and pyoveridine.

647 The extreme adaptability and excellent survival of *Pseudomonas* species have been
648 claimed to originate from the plasticity of gene expression facilitated by the high number of
649 transcriptional regulators encoded in their genomes [83,84]. ParB excess leads to the
650 induction of several genes encoding known and putative transcriptional regulators (Table 4).
651 Among them is *PA2432* encoding the bistable response regulator BexR [67]. Bistability refers
652 to a phenotypic heterogeneity within an isogenic population which allows a fraction of cells to
653 survive in otherwise lethal conditions [85]. The BexR regulon comprises a diverse set of up-
654 and down- regulated genes related to virulence and quorum sensing [67]. Importantly, the
655 *bexR* induction in response to ParB excess is highly reproducible and approaches the ~10-fold
656 induction maximum found in the subset of cells which have switched on the BexR regulon
657 [67]. The mobilization of pKGB9 (*araBAD*p-*parB*) and pKGB8 (*araBAD*p) plasmids into the
658 test strain PAO1161::*bexR*p-*lacZ* with "OFF" phenotype demonstrated "ON" state of *bexR*p
659 in nearly all conjugants with pKGB9 and in a tiny fraction of conjugants with pKGB8
660 (<0.1%). This confirms that the ParB excess induces the *bexR* gene in all cells rather than in a
661 specific subpopulation only. So far the mechanism of *bexR* induction in response to ParB
662 excess remains unknown.

bioRxiv preprint doi: https://doi.org/10.1101/151340; this version posted June 20, 2017. The copyright holder for this preprint (which was not certified by peer review) is the author/funder, who has granted bioRxiv a license to display the preprint in perpetuity. It is made available under aCC-BY-NC-ND 4.0 International license.

663 Our study also revealed that ParB excess leads to the induction of bacteriophage and
664 pyocin encoding genes, which in *P. aeruginosa* are hallmarks of the SOS response [62,86].
665 Whereas the SOS response had initially been linked exclusively to DNA damage signals, it
666 was later established to be part of a broad stress reaction [87,88]. SOS response is tightly
667 connected to cell growth inhibition, cell-cycle checkpoints and even programmed cell death
668 [89–91]. The phage- and pyocins-related genes are among the genes responding similarly to
669 the *parB* deficiency and ParB excess (Table S4), suggesting that any imbalance in the
670 ParA/ParB/*parS* system may trigger SOS response.

671 Altogether, our data indicate that the level of partitioning protein ParB in *P.*
672 *aeruginosa* influences the expression of numerous genes including those involved in
673 virulence, stress response and quorum sensing. Further studies are needed to decipher whether
674 these effects are a direct result of ParB binding to DNA (specific or non-specific), interactions
675 with other proteins or are caused indirectly, for example by topological changes.

676 **Acknowledgements**

677 We thank dr Paulina Jęcz for the construction of pPJB132. This work was supported by the
678 Polish National Science Centre grant no 2013/11/B/NZ2/02555 awarded to GJB.

679 **References**

680 1. Salje J. Plasmid segregation: how to survive as an extra piece of DNA. Crit Rev
681 Biochem Mol Biol. 2010;45: 296–317. doi:10.3109/10409238.2010.494657

682 2. Baxter JC, Funnell BE. Plasmid partition mechanisms. Microbiol Spectr. 2014;2.
683 doi:10.1128/microbiolspec.PLAS-0023-2014

684 3. Gerdes K, Howard M, Szardenings F. Pushing and pulling in prokaryotic DNA
685 segregation. Cell. 2010;141: 927–942. doi:10.1016/j.cell.2010.05.033

bioRxiv preprint doi: https://doi.org/10.1101/151340; this version posted June 20, 2017. The copyright holder for this preprint (which was not certified by peer review) is the author/funder, who has granted bioRxiv a license to display the preprint in perpetuity. It is made available under aCC-BY-NC-ND 4.0 International license.

4. Gerdes K, Møller-Jensen J, Jensen RB. Plasmid and chromosome partitioning: surprises from phylogeny. Mol Microbiol. 2000;37: 455–466. doi:10.1046/j.1365-2958.2000.01975.x

5. Funnell BE. ParB partition proteins: complex formation and spreading at bacterial and plasmid centromeres. Mol Recognit. 2016; 44. doi:10.3389/fmolb.2016.00044

6. Yamaichi Y, Niki H. Active segregation by the *Bacillus subtilis* partitioning system in *Escherichia coli*. Proc Natl Acad Sci. 2000;97: 14656–14661. doi:10.1073/pnas.97.26.14656

7. Livny J, Yamaichi Y, Waldor MK. Distribution of centromere-like *parS* sites in bacteria: insights from comparative genomics. J Bacteriol. 2007;189: 8693–8703. doi:10.1128/JB.01239-07

8. Mohl DA, Gober JW. Cell cycle–dependent polar localization of chromosome partitioning proteins in *Caulobacter crescentus*. Cell. 1997;88: 675–684. doi:10.1016/S0092-8674(00)81910-8

9. Iniesta AA. ParABS system in chromosome partitioning in the bacterium *Myxococcus xanthus*. PLOS ONE. 2014;9: e86897. doi:10.1371/journal.pone.0086897

10. Ireton K, Gunther NW, Grossman AD. Spo0J is required for normal chromosome segregation as well as the initiation of sporulation in *Bacillus subtilis*. J Bacteriol. 1994;176: 5320–5329.

11. Sharpe ME, Errington J. The *Bacillus subtilis soj-spo0J* locus is required for a centromere-like function involved in prespore chromosome partitioning. Mol Microbiol. 1996;21: 501–509. doi:10.1111/j.1365-2958.1996.tb02559.x

bioRxiv preprint doi: https://doi.org/10.1101/151340; this version posted June 20, 2017. The copyright holder for this preprint (which was not certified by peer review) is the author/funder, who has granted bioRxiv a license to display the preprint in perpetuity. It is made available under aCC-BY-NC-ND 4.0 International license.

12. Lewis PJ, Errington J. Direct evidence for active segregation of *oriC* regions of the *Bacillus subtilis* chromosome and co-localization with the Spo0J partitioning protein. Mol Microbiol. 1997;25: 945–954.

13. Lin DC-H, Grossman AD. Identification and characterization of a bacterial chromosome partitioning site. Cell. 1998;92: 675–685. doi:10.1016/S0092-8674(00)81135-6

14. Kim HJ, Calcutt MJ, Schmidt FJ, Chater KF. Partitioning of the linear chromosome during sporulation of *Streptomyces coelicolor* A3(2) involves an *oriC*-linked *parAB* locus. J Bacteriol. 2000;182: 1313–1320.

15. Fogel MA, Waldor MK. A dynamic, mitotic-like mechanism for bacterial chromosome segregation. Genes Dev. 2006;20: 3269–3282. doi:10.1101/gad.1496506

16. Saint-Dic D, Frushour BP, Kehrl JH, Kahng LS. A parA homolog selectively influences positioning of the large chromosome origin in *Vibrio cholerae*. J Bacteriol. 2006;188: 5626–5631. doi:10.1128/JB.00250-06

17. Bartosik AA, Mierzejewska J, Thomas CM, Jagura-Burdzy G. ParB deficiency in *Pseudomonas aeruginosa* destabilizes the partner protein ParA and affects a variety of physiological parameters. Microbiology. 2009;155: 1080–1092. doi:10.1099/mic.0.024661-0

18. Lasocki K, Bartosik AA, Mierzejewska J, Thomas CM, Jagura-Burdzy G. Deletion of the *parA* (*soj*) homologue in *Pseudomonas aeruginosa* causes ParB instability and affects growth rate, chromosome segregation, and motility. J Bacteriol. 2007;189: 5762–5772. doi:10.1128/JB.00371-07

bioRxiv preprint doi: https://doi.org/10.1101/151340; this version posted June 20, 2017. The copyright holder for this preprint (which was not certified by peer review) is the author/funder, who has granted bioRxiv a license to display the preprint in perpetuity. It is made available under aCC-BY-NC-ND 4.0 International license.

729 19. Vallet-Gely I, Boccard F. Chromosomal organization and segregation in *Pseudomonas*
730 *aeruginosa*. PLOS Genet. 2013;9: e1003492. doi:10.1371/journal.pgen.1003492

731 20. Gruber S, Errington J. Recruitment of condensin to replication origin regions by
732 ParB/Spo0J promotes chromosome segregation in *B. subtilis*. Cell. 2009;137: 685–696.
733 doi:10.1016/j.cell.2009.02.035

734 21. Sullivan NL, Marquis KA, Rudner DZ. Recruitment of SMC by ParB-*parS* organizes the
735 origin region and promotes efficient chromosome segregation. Cell. 2009;137: 697–707.
736 doi:10.1016/j.cell.2009.04.044

737 22. Minnen A, Attaiech L, Thon M, Gruber S, Veening J-W. SMC is recruited to *oriC* by
738 ParB and promotes chromosome segregation in *Streptococcus pneumoniae*. Mol
739 Microbiol. 2011;81: 676–688. doi:10.1111/j.1365-2958.2011.07722.x

740 23. Lee PS, Grossman AD. The chromosome partitioning proteins Soj (ParA) and Spo0J
741 (ParB) contribute to accurate chromosome partitioning, separation of replicated sister
742 origins, and regulation of replication initiation in *Bacillus subtilis*. Mol Microbiol.
743 2006;60: 853–869. doi:10.1111/j.1365-2958.2006.05140.x

744 24. Murray H, Errington J. Dynamic control of the DNA replication initiation protein DnaA
745 by Soj/ParA. Cell. 2008;135: 74–84. doi:10.1016/j.cell.2008.07.044

746 25. Scholefield G, Whiting R, Errington J, Murray H. Spo0J regulates the oligomeric state of
747 Soj to trigger its switch from an activator to an inhibitor of DNA replication initiation.
748 Mol Microbiol. 2011;79: 1089–1100. doi:10.1111/j.1365-2958.2010.07507.x

bioRxiv preprint doi: https://doi.org/10.1101/151340; this version posted June 20, 2017. The copyright holder for this preprint (which was not certified by peer review) is the author/funder, who has granted bioRxiv a license to display the preprint in perpetuity. It is made available under aCC-BY-NC-ND 4.0 International license.

749 26. Figge RM, Easter J, Gober JW. Productive interaction between the chromosome
750 partitioning proteins, ParA and ParB, is required for the progression of the cell cycle in
751 *Caulobacter crescentus*. Mol Microbiol. 2003;47: 1225–1237.

752 27. Hajduk IV, Rodrigues CDA, Harry EJ. Connecting the dots of the bacterial cell cycle:
753 coordinating chromosome replication and segregation with cell division. Semin Cell Dev
754 Biol. 2016;53: 2–9. doi:10.1016/j.semcdb.2015.11.012

755 28. Donczew M, Mackiewicz P, Wróbel A, Flärdh K, Zakrzewska-Czerwińska J,
756 Jakimowicz D. ParA and ParB coordinate chromosome segregation with cell elongation
757 and division during *Streptomyces sporulation*. Open Biol. 2016;6: 150263.
758 doi:10.1098/rsob.150263

759 29. Murray H, Ferreira H, Errington J. The bacterial chromosome segregation protein Spo0J
760 spreads along DNA from *parS* nucleation sites. Mol Microbiol. 2006;61: 1352–1361.
761 doi:10.1111/j.1365-2958.2006.05316.x

762 30. Broedersz CP, Wang X, Meir Y, Loparo JJ, Rudner DZ, Wingreen NS. Condensation
763 and localization of the partitioning protein ParB on the bacterial chromosome. Proc Natl
764 Acad Sci. 2014;111: 8809–8814. doi:10.1073/pnas.1402529111

765 31. Graham TGW, Wang X, Song D, Etson CM, Oijen AM van, Rudner DZ, et al. ParB
766 spreading requires DNA bridging. Genes Dev. 2014; doi:10.1101/gad.242206.114

767 32. Taylor JA, Pastrana CL, Butterer A, Pernstich C, Gwynn EJ, Sobott F, et al. Specific and
768 non-specific interactions of ParB with DNA: implications for chromosome segregation.
769 Nucleic Acids Res. 2015;43: 719–731. doi:10.1093/nar/gku1295

bioRxiv preprint doi: https://doi.org/10.1101/151340; this version posted June 20, 2017. The copyright holder for this preprint (which was not certified by peer review) is the author/funder, who has granted bioRxiv a license to display the preprint in perpetuity. It is made available under aCC-BY-NC-ND 4.0 International license.

770 33. Lagage V, Boccard F, Vallet-Gely I. Regional control of chromosome segregation in
771 *Pseudomonas aeruginosa*. PLOS Genet. 2016;12: e1006428.
772 doi:10.1371/journal.pgen.1006428

773 34. Baek JH, Rajagopala SV, Chattoraj DK. Chromosome segregation proteins of *Vibrio*
774 *cholerae* as transcription regulators. mBio. 2014;5: e01061-14.
775 doi:10.1128/mBio.01061-14

776 35. Breier AM, Grossman AD. Whole-genome analysis of the chromosome partitioning and
777 sporulation protein Spo0J (ParB) reveals spreading and origin-distal sites on the *Bacillus*
778 *subtilis* chromosome. Mol Microbiol. 2007;64: 703–718. doi:10.1111/j.1365-
779 2958.2007.05690.x

780 36. Attaiech L, Minnen A, Kjos M, Gruber S, Veening J-W. The ParB-*parS* chromosome
781 segregation system modulates competence development in *Streptococcus pneumoniae*.
782 mBio. 2015;6: e00662-15. doi:10.1128/mBio.00662-15

783 37. Bartosik AA, Lasocki K, Mierzejewska J, Thomas CM, Jagura-Burdzy G. ParB of
784 *Pseudomonas aeruginosa*: interactions with its partner ParA and its target *parS* and
785 specific effects on bacterial growth. J Bacteriol. 2004;186: 6983–6998.
786 doi:10.1128/JB.186.20.6983-6998.2004

787 38. Jecz P, Bartosik AA, Glabski K, Jagura-Burdzy G. A Single *parS* Sequence from the
788 cluster of four sites closest to *oriC* is necessary and sufficient for proper chromosome
789 segregation in *Pseudomonas aeruginosa*. PLOS ONE. 2015;10: e0120867.
790 doi:10.1371/journal.pone.0120867

791 39. Bartosik AA, Glabski K, Jecz P, Mikulska S, Fogtman A, Koblowska M, et al.
792 Transcriptional profiling of ParA and ParB Mutants in actively dividing cells of an

bioRxiv preprint doi: https://doi.org/10.1101/151340; this version posted June 20, 2017. The copyright holder for this preprint (which was not certified by peer review) is the author/funder, who has granted bioRxiv a license to display the preprint in perpetuity. It is made available under aCC-BY-NC-ND 4.0 International license.

793 opportunistic human pathogen *Pseudomonas aeruginosa*. PLOS ONE. 2014;9: e87276.
794 doi:10.1371/journal.pone.0087276

795 40. Kusiak M, Gapczynska A, Plochocka D, Thomas CM, Jagura-Burdzy G. Binding and
796 spreading of ParB on DNA determine its biological function in *Pseudomonas*
797 *aeruginosa*. J Bacteriol. 2011;193: 3342–3355. doi:10.1128/JB.00328-11

798 41. Mierzejewska J, Bartosik AA, Macioszek M, Płochocka D, Thomas CM, Jagura-Burdzy
799 G. Identification of C-terminal hydrophobic residues important for dimerization and all
800 known functions of ParB of *Pseudomonas aeruginosa*. Microbiol Read Engl. 2012;158:
801 1183–1195. doi:10.1099/mic.0.056234-0

802 42. Miller JH. Experiments in molecular genetics. 1972; Cold Spring Harbor Laboratory
803 Press, Cold Spring Harbor, NY

804 43. Hanahan D. Studies on transformation of *Escherichia coli* with plasmids. J Mol Biol.
805 1983;166: 557–580. doi:10.1016/S0022-2836(83)80284-8

806 44. Simon R, Priefer U, Pühler A. A broad host range mobilization system for in vivo
807 genetic engineering: transposon mutagenesis in gram negative bacteria. Nat Biotechnol.
808 1983;1: 784–791. doi:10.1038/nbt1183-784

809 45. Irani VR, Rowe JJ. Enhancement of transformation in *Pseudomonas aeruginosa* PAO1
810 by Mg2+ and heat. BioTechniques. 1997;22: 54–56.

811 46. Sambrook J, Fritsch EF, Maniatis T. Molecular cloning: a laboratory manual. Cold
812 Spring Harbor Laboratory; 1989.

813 47. Ludwiczak M, Dolowy P, Markowska A, Szarlak J, Kulinska A, Jagura-Burdzy G.
814 Global transcriptional regulator KorC coordinates expression of three backbone modules

bioRxiv preprint doi: https://doi.org/10.1101/151340; this version posted June 20, 2017. The copyright holder for this preprint (which was not certified by peer review) is the author/funder, who has granted bioRxiv a license to display the preprint in perpetuity. It is made available under aCC-BY-NC-ND 4.0 International license.

of the broad-host-range RA3 plasmid from IncU incompatibility group. Plasmid. 2013;70: 131–145. doi:10.1016/j.plasmid.2013.03.007

48. El-Sayed AK, Hothersall J, Thomas CM. Quorum-sensing-dependent regulation of biosynthesis of the polyketide antibiotic mupirocin in *Pseudomonas fluorescens* NCIMB 10586. Microbiology. 2001;147: 2127–2139. doi:10.1099/00221287-147-8-2127

49. Guzman LM, Belin D, Carson MJ, Beckwith J. Tight regulation, modulation, and high-level expression by vectors containing the arabinose PBAD promoter. J Bacteriol. 1995;177: 4121–4130.

50. Marx CJ, Lidstrom ME. Development of improved versatile broad-host-range vectors for use in methylotrophs and other Gram-negative bacteria. Microbiol Read Engl. 2001;147: 2065–2075. doi:10.1099/00221287-147-8-2065

51. Reece KS, Phillips GJ. New plasmids carrying antibiotic-resistance cassettes. Gene. 1995;165: 141–142. doi:10.1016/0378-1119(95)00529-F

52. Soukas A, Cohen P, Socci ND, Friedman JM. Leptin-specific patterns of gene expression in white adipose tissue. Genes Dev. 2000;14: 963–980. doi:10.1101/gad.14.8.963

53. Saeed AI, Sharov V, White J, Li J, Liang W, Bhagabati N, et al. TM4: a free, open-source system for microarray data management and analysis. BioTechniques. 2003;34: 374–378.

54. Pfaffl MW. A new mathematical model for relative quantification in real-time RT-PCR. Nucleic Acids Res. 2001;29: e45.

bioRxiv preprint doi: https://doi.org/10.1101/151340; this version posted June 20, 2017. The copyright holder for this preprint (which was not certified by peer review) is the author/funder, who has granted bioRxiv a license to display the preprint in perpetuity. It is made available under aCC-BY-NC-ND 4.0 International license.

836 55. O'Toole GA, Kolter R. Initiation of biofilm formation in *Pseudomonas fluorescens*
837 WCS365 proceeds via multiple, convergent signalling pathways: a genetic analysis. Mol
838 Microbiol. 1998;28: 449–461. doi:10.1046/j.1365-2958.1998.00797.x

839 56. Kovach ME, Elzer PH, Hill DS, Robertson GT, Farris MA, Roop RM, et al. Four new
840 derivatives of the broad-host-range cloning vector pBBR1MCS, carrying different
841 antibiotic-resistance cassettes. Gene. 1995;166: 175–176.

842 57. Winsor GL, Lo R, Ho Sui SJ, Ung KSE, Huang S, Cheng D, et al. *Pseudomonas*
843 *aeruginosa* genome database and PseudoCAP: facilitating community-based, continually
844 updated, genome annotation. Nucleic Acids Res. 2005;33: D338-343.
845 doi:10.1093/nar/gki047

846 58. Yamamoto M, Ueda A, Kudo M, Matsuo Y, Fukushima J, Nakae T, et al. Role of MexZ
847 and PA5471 in transcriptional regulation of *mexXY* in *Pseudomonas aeruginosa*.
848 Microbiology. 2009;155: 3312–3321. doi:10.1099/mic.0.028993-0

849 59. Hay T, Fraud S, Lau CH-F, Gilmour C, Poole K. Antibiotic inducibility of the *mexXY*
850 multidrug efflux operon of *Pseudomonas aeruginosa*: involvement of the MexZ anti-
851 repressor ArmZ. PLoS ONE. 2013;8: e56858. doi:10.1371/journal.pone.0056858

852 60. Mac Aogáin M, Mooij MJ, McCarthy RR, Plower E, Wang YP, Tian ZX, et al. The non-
853 classical ArsR-family repressor PyeR (PA4354) modulates biofilm formation in
854 *Pseudomonas aeruginosa*. Microbiol Read Engl. 2012;158: 2598–2609.
855 doi:10.1099/mic.0.058636-0

856 61. Hoffman LR, D'Argenio DA, MacCoss MJ, Zhang Z, Jones RA, Miller SI.
857 Aminoglycoside antibiotics induce bacterial biofilm formation. Nature. 2005;436: 1171–
858 1175. doi:10.1038/nature03912

bioRxiv preprint doi: https://doi.org/10.1101/151340; this version posted June 20, 2017. The copyright holder for this preprint (which was not certified by peer review) is the author/funder, who has granted bioRxiv a license to display the preprint in perpetuity. It is made available under aCC-BY-NC-ND 4.0 International license.

859 62. Cirz RT, O'Neill BM, Hammond JA, Head SR, Romesberg FE. Defining the
860 *Pseudomonas aeruginosa* SOS response and its role in the global response to the
861 antibiotic ciprofloxacin. J Bacteriol. 2006;188: 7101–7110. doi:10.1128/JB.00807-06

862 63. McFarland KA, Dolben EL, LeRoux M, Kambara TK, Ramsey KM, Kirkpatrick RL, et
863 al. A self-lysis pathway that enhances the virulence of a pathogenic bacterium. Proc Natl
864 Acad Sci. 2015;112: 8433–8438. doi:10.1073/pnas.1506299112

865 64. Matsui H, Sano Y, Ishihara H, Shinomiya T. Regulation of pyocin genes in
866 *Pseudomonas aeruginosa* by positive (*prtN*) and negative (*prtR*) regulatory genes. J
867 Bacteriol. 1993;175: 1257–1263.

868 65. Hood RD, Singh P, Hsu F, Güvener T, Carl MA, Trinidad RRS, et al. A type VI
869 secretion system of *Pseudomonas aeruginosa* targets a toxin to bacteria. Cell Host
870 Microbe. 2010;7: 25–37. doi:10.1016/j.chom.2009.12.007

871 66. Lesic B, Starkey M, He J, Hazan R, Rahme LG. Quorum sensing differentially regulates
872 *Pseudomonas aeruginosa* type VI secretion locus I and homologous loci II and III,
873 which are required for pathogenesis. Microbiol Read Engl. 2009;155: 2845–2855.
874 doi:10.1099/mic.0.029082-0

875 67. Turner KH, Vallet-Gely I, Dove SL. Epigenetic control of virulence gene expression in
876 *Pseudomonas aeruginosa* by a LysR-type transcription regulator. PLOS Genet. 2009;5:
877 e1000779. doi:10.1371/journal.pgen.1000779

878 68. Wade DS, Calfee MW, Rocha ER, Ling EA, Engstrom E, Coleman JP, et al. Regulation
879 of Pseudomonas quinolone signal synthesis in *Pseudomonas aeruginosa*. J Bacteriol.
880 2005;187: 4372–4380. doi:10.1128/JB.187.13.4372-4380.2005

bioRxiv preprint doi: https://doi.org/10.1101/151340; this version posted June 20, 2017. The copyright holder for this preprint (which was not certified by peer review) is the author/funder, who has granted bioRxiv a license to display the preprint in perpetuity. It is made available under aCC-BY-NC-ND 4.0 International license.

881 69. Sams T, Baker Y, Hodgkinson J, Gross J, Spring D, Welch M. The Pseudomonas
882 quinolone signal (PQS). Isr J Chem. 2016;56: 282–294. doi:10.1002/ijch.201400128

883 70. Déziel E, Gopalan S, Tampakaki AP, Lépine F, Padfield KE, Saucier M, et al. The
884 contribution of MvfR to *Pseudomonas aeruginosa* pathogenesis and quorum sensing
885 circuitry regulation: multiple quorum sensing-regulated genes are modulated without
886 affecting *lasRI*, *rhlRI* or the production of N-acyl- l-homoserine lactones. Mol
887 Microbiol. 2005;55: 998–1014. doi:10.1111/j.1365-2958.2004.04448.x

888 71. Xiao G, He J, Rahme LG. Mutation analysis of the *Pseudomonas aeruginosa mvfR* and
889 *pqsABCDE* gene promoters demonstrates complex quorum-sensing circuitry. Microbiol
890 Read Engl. 2006;152: 1679–1686. doi:10.1099/mic.0.28605-0

891 72. Zheng P, Sun J, Geffers R, Zeng A-P. Functional characterization of the gene *PA2384* in
892 large-scale gene regulation in response to iron starvation in *Pseudomonas aeruginosa*. J
893 Biotechnol. 2007;132: 342–352. doi:10.1016/j.jbiotec.2007.08.013

894 73. Mao X, Ma Q, Zhou C, Chen X, Zhang H, Yang J, et al. DOOR 2.0: presenting operons
895 and their functions through dynamic and integrated views. Nucleic Acids Res. 2014;42:
896 D654-659. doi:10.1093/nar/gkt1048

897 74. V. Solovyev, A Salamov. Automatic annotation of microbial genomes and metagenomic
898 sequences. In: Li RW, editor. Metagenomics and its applications in agriculture,
899 biomedicine and environmental studies. Nova Science Publishers; 2011. pp. 61-78.

900 75. Wang X, Le TBK, Lajoie BR, Dekker J, Laub MT, Rudner DZ. Condensin promotes the
901 juxtaposition of DNA flanking its loading site in *Bacillus subtilis*. Genes Dev. 2015;29:
902 1661–1675. doi:10.1101/gad.265876.115

bioRxiv preprint doi: https://doi.org/10.1101/151340; this version posted June 20, 2017. The copyright holder for this preprint (which was not certified by peer review) is the author/funder, who has granted bioRxiv a license to display the preprint in perpetuity. It is made available under aCC-BY-NC-ND 4.0 International license.

903 76. Hittle LE, Powell DA, Jones JW, Tofigh M, Goodlett DR, Moskowitz SM, et al. Site-
904 specific activity of the acyltransferases HtrB1 and HtrB2 in *Pseudomonas aeruginosa*
905 lipid A biosynthesis. Pathog Dis. 2015;73. doi:10.1093/femspd/ftv053

906 77. Wang B, Li B, Liang Y, Li J, Gao L, Chen L, et al. Pleiotropic effects of temperature-
907 regulated 2-OH-lauroytransferase (PA0011) on *Pseudomonas aeruginosa* antibiotic
908 resistance, virulence and type III secretion system. Microb Pathog. 2016;91: 5–17.
909 doi:10.1016/j.micpath.2015.11.003

910 78. Shen L, Ma Y, Liang H. Characterization of a novel gene related to antibiotic
911 susceptibility in *Pseudomonas aeruginosa*. J Antibiot (Tokyo). 2012;65: 59–65.
912 doi:10.1038/ja.2011.111

913 79. Liang Y, Guo Z, Gao L, Guo Q, Wang L, Han Y, et al. The role of the temperature-
914 regulated acyltransferase (PA3242) on growth, antibiotic resistance and virulence in
915 *Pseudomonas aeruginosa*. Microb Pathog. 2016;101: 126–135.
916 doi:10.1016/j.micpath.2016.09.019

917 80. Evensen G, Seeberg E. Adaptation to alkylation resistance involves the induction of a
918 DNA glycosylase. Nature. 1982;296: 773–775.

919 81. Hengge R. Principles of c-di-GMP signalling in bacteria. Nat Rev Microbiol. 2009;7:
920 263–273. doi:10.1038/nrmicro2109

921 82. Valentini M, Filloux A. Biofilms and Cyclic di-GMP (c-di-GMP) Signaling: lessons
922 from *Pseudomonas aeruginosa* and other bacteria. J Biol Chem. 2016;291: 12547–
923 12555. doi:10.1074/jbc.R115.711507

bioRxiv preprint doi: https://doi.org/10.1101/151340; this version posted June 20, 2017. The copyright holder for this preprint (which was not certified by peer review) is the author/funder, who has granted bioRxiv a license to display the preprint in perpetuity. It is made available under aCC-BY-NC-ND 4.0 International license.

924 83. Stover CK, Pham XQ, Erwin AL, Mizoguchi SD, Warrener P, Hickey MJ, et al.
925 Complete genome sequence of *Pseudomonas aeruginosa* PAO1, an opportunistic
926 pathogen. Nature. 2000;406: 959–964. doi:10.1038/35023079

927 84. Potvin E, Sanschagrin F, Levesque RC. Sigma factors in *Pseudomonas aeruginosa*.
928 FEMS Microbiol Rev. 2008;32: 38–55. doi:10.1111/j.1574-6976.2007.00092.x

929 85. Veening J-W, Smits WK, Kuipers OP. Bistability, epigenetics, and bet-hedging in
930 bacteria. Annu Rev Microbiol. 2008;62: 193–210.
931 doi:10.1146/annurev.micro.62.081307.163002

932 86. Penterman J, Singh PK, Walker GC. Biological cost of pyocin production during the
933 SOS response in *Pseudomonas aeruginosa*. J Bacteriol. 2014;196: 3351–3359.
934 doi:10.1128/JB.01889-14

935 87. Kreuzer KN. DNA damage responses in prokaryotes: regulating gene expression,
936 modulating growth patterns, and manipulating replication forks. Cold Spring Harb
937 Perspect Biol. 2013;5: a012674. doi:10.1101/cshperspect.a012674

938 88. Baharoglu Z, Mazel D. SOS, the formidable strategy of bacteria against aggressions.
939 FEMS Microbiol Rev. 2014;38: 1126–1145. doi:10.1111/1574-6976.12077

940 89. Modell JW, Hopkins AC, Laub MT. A DNA damage checkpoint in *Caulobacter*
941 *crescentus* inhibits cell division through a direct interaction with FtsW. Genes Dev.
942 2011;25: 1328–1343. doi:10.1101/gad.2038911

943 90. Erental A, Kalderon Z, Saada A, Smith Y, Engelberg-Kulka H. Apoptosis-like death, an
944 extreme SOS response in *Escherichia coli*. mBio. 2014;5: e01426-14.
945 doi:10.1128/mBio.01426-14

bioRxiv preprint doi: https://doi.org/10.1101/151340; this version posted June 20, 2017. The copyright holder for this preprint (which was not certified by peer review) is the author/funder, who has granted bioRxiv a license to display the preprint in perpetuity. It is made available under aCC-BY-NC-ND 4.0 International license.

946 91. Nariya H, Inouye M. MazF, an mRNA interferase, mediates programmed cell death
947 during multicellular *Myxococcus* development. Cell. 2008;132: 55–66.
948 doi:10.1016/j.cell.2007.11.044

949

950 **Supporting information captions**

951 **S1 Figure.** Analysis of genes identified as altered in ParB+ *vs* EV but not ParB+++ *vs* EV.
952 Abbreviation ParB+ corresponds to PAO1161 (pKGB9 *araBAD*p-*parB*) strain grown without
953 arabinose, EV corresponds to PAO1161 (pKGB8 *araBAD*p) grown with arabinose and
954 ParB+++ for PAO1161 (pKGB9 *araBAD*p-*parB*) cells grown with arabinose. (**A**) Fold
955 change- and *p*- values for the 35 genes in ParB+ vs EV and ParB+++ vs EV analysis. First
956 subgroup of genes with -1.6> FC >-2 or 1.6< FC <2 and *p*-value <0.05 in ParB+++ vs EV
957 comparison is indicated in green. The second subgroup of genes with 0.05< *p*-value <0.1 in
958 ParB+++ vs EV comparison is indicated in blue. The third subgroup of genes with *p*-value
959 >0.1 and -1.5< FC < 1.5 is left uncoloured. Genes in operons are marked with arrows. (**B**)
960 Impact of arabinose on the expression of selected genes. PAO1161 (pKGB8 *araBAD*p) cells
961 were grown in L broth containing chloramphenicol with or without 0.02% arabinose. RT-
962 qPCR was performed cDNA synthesized on RNA isolated from cells harvested at OD_{600} 0.5.
963 Data represent mean ±SD from three biological replicates. Expression values for all genes are
964 shown relative to the cells from cultures without arabinose. * - *p*-value < 0.05 in two-sided
965 Student's *t*-test assuming equal variance.

966 **S1 Table**. Oligonucleotides used in this work.

967 **S2 Table**. Transcriptomic changes between analyzed PAO1161 strains. (**A)** Comparison of
968 PAO1161 (pKGB8 *araBAD*p) (EV) *vs* PAO1161 (WT). (**B)** Comparison of PAO1161
969 (pKGB9 *araBAD*p-*parB*) grown without arabinose (ParB+) *vs* EV. (**C)** Comparison of

bioRxiv preprint doi: https://doi.org/10.1101/151340; this version posted June 20, 2017. The copyright holder for this preprint (which was not certified by peer review) is the author/funder, who has granted bioRxiv a license to display the preprint in perpetuity. It is made available under aCC-BY-NC-ND 4.0 International license.

970 PAO1161(pKGB9 *araBAD*p-*parB*) grown with 0.02% arabinose (ParB+++) *vs* EV. (**D**) List
971 of 211 loci displaying altered expression in ParB overproducing cells.

972 **S3 Table**. K-means clustering of ParB dependent loci. Mean levels of transcripts for all loci
973 are shown relative to PAO1161 (pKGB8 *araBAD*p).

974 **S4 Table**. Genes with altered expression in response to ParB deficiency (PAO1161 $parB_{null}$)
975 and ParB overproduction [PAO1161 (pKGB9 *araBAD*p-*parB*) grown with or without 0.02%
976 arabinose vs PAO1161 (pKGB8 *araBAD*p)].

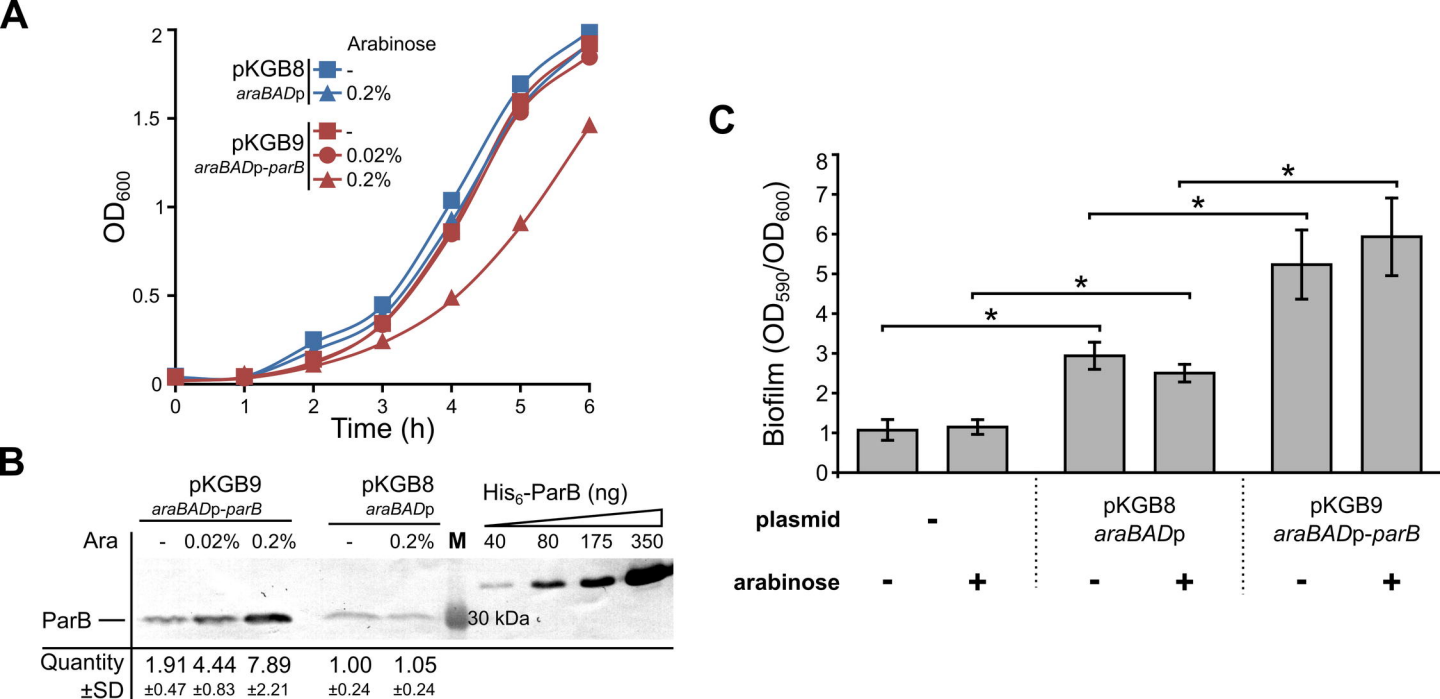
A
Arabinose
pKGB8
araBADp
-
0.2%
pKGB9
araBADp-parB
-
0.02%
0.2%
OD600
Time (h)
B
pKGB9
araBADp-parB
pKGB8
araBADp
His6-ParB (ng)
Ara
- 0.02% 0.2%
- 0.2%
M
40 80 175 350
ParB
30 kDa
Quantity
1.91 4.44 7.89
1.00 1.05
±SD
±0.47 ±0.83 ±2.21
±0.24 ±0.24
C
Biofilm (OD590/OD600)
plasmid
-
pKGB8
araBADp
pKGB9
araBADp-parB
arabinose
- + - + - +

A

	Total	UP	DOWN
EV *vs* WT	78	33	45
ParB+ *vs* EV	157	114	43
ParB+++ *vs* EV	176	129	47

B

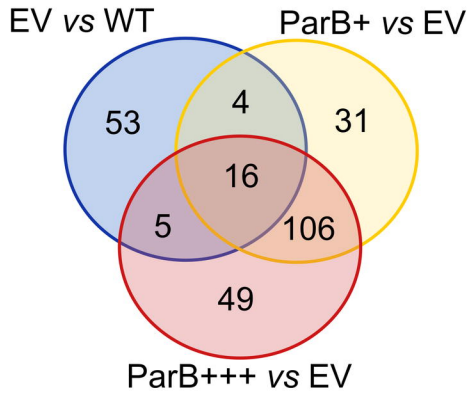

C

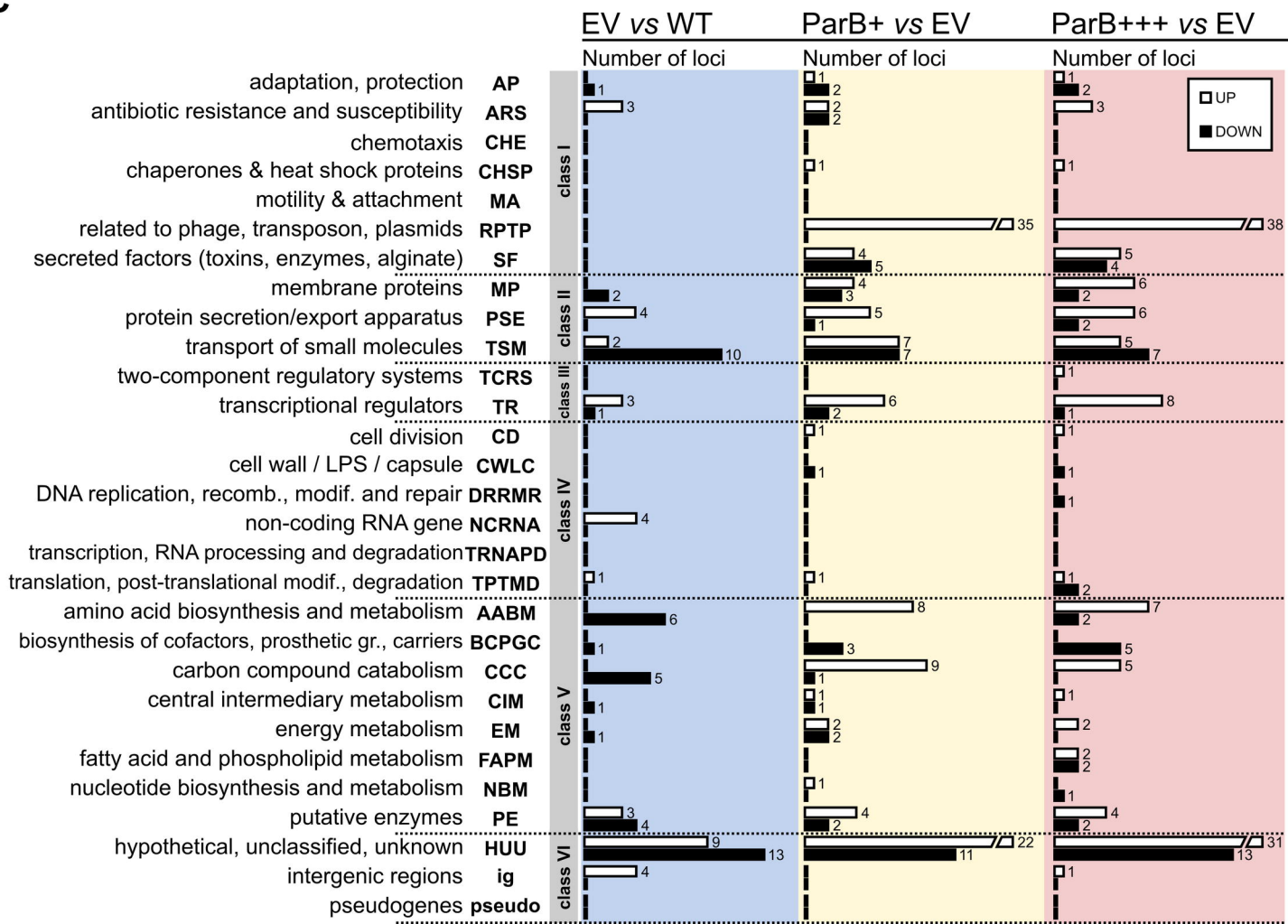

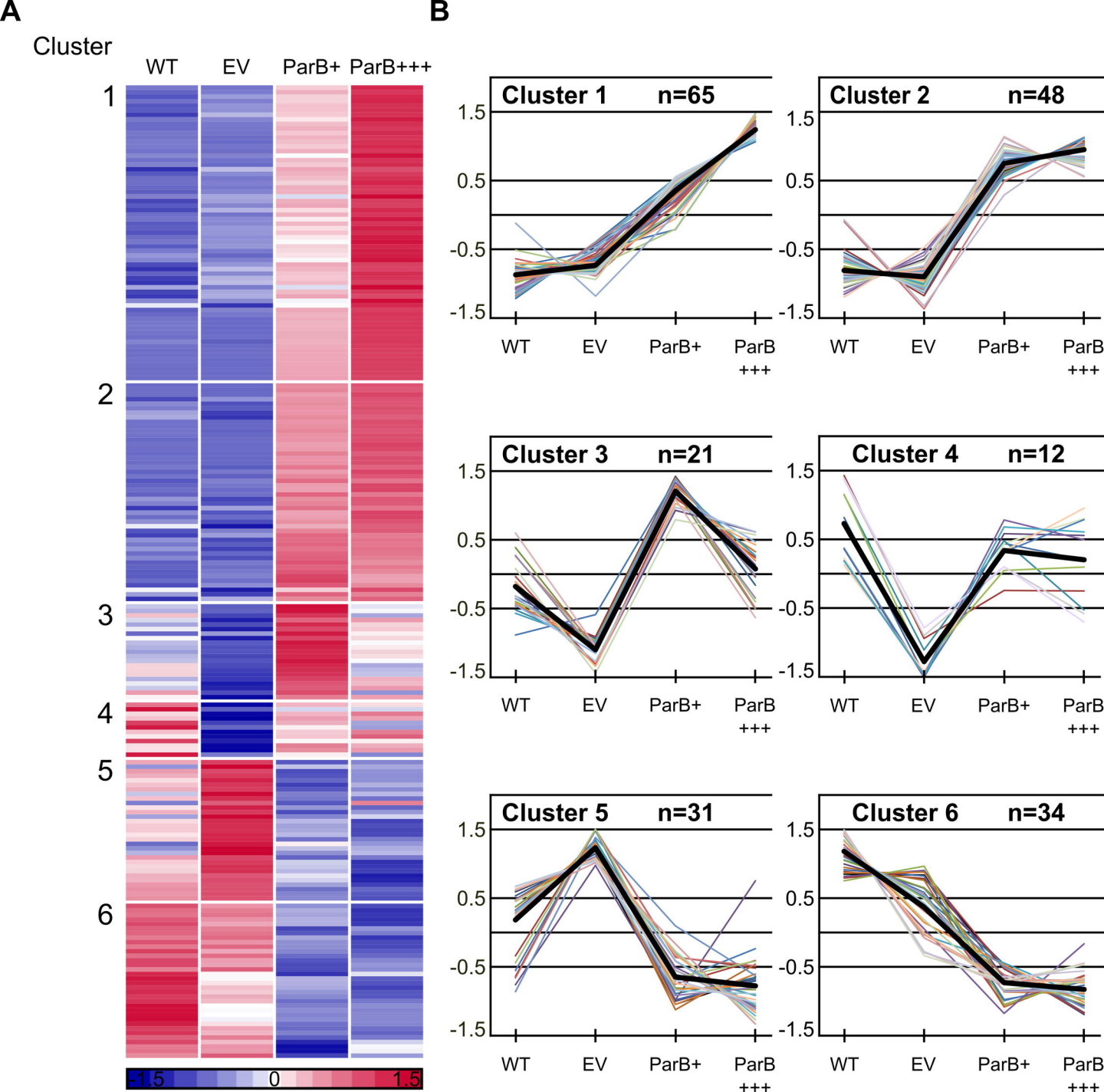
A
Cluster
WT
EV
ParB+
ParB+++
1
2
3
4
5
6
-1.5
0
1.5
B
Cluster 1 n=65
Cluster 2 n=48
Cluster 3 n=21
Cluster 4 n=12
Cluster 5 n=31
Cluster 6 n=34
1.5
0.5
-0.5
-1.5
WT
EV
ParB+
ParB +++

PAO1161::*bexR*p-*lacZ*

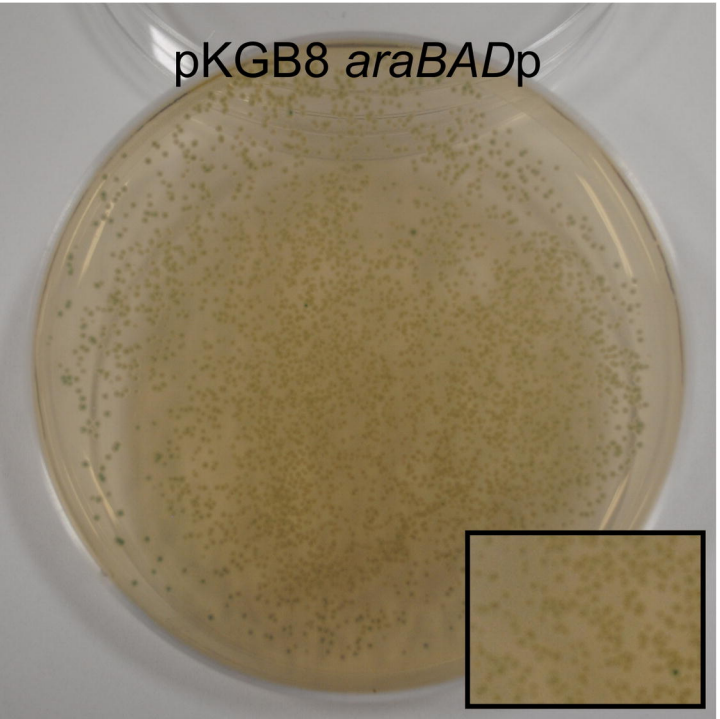

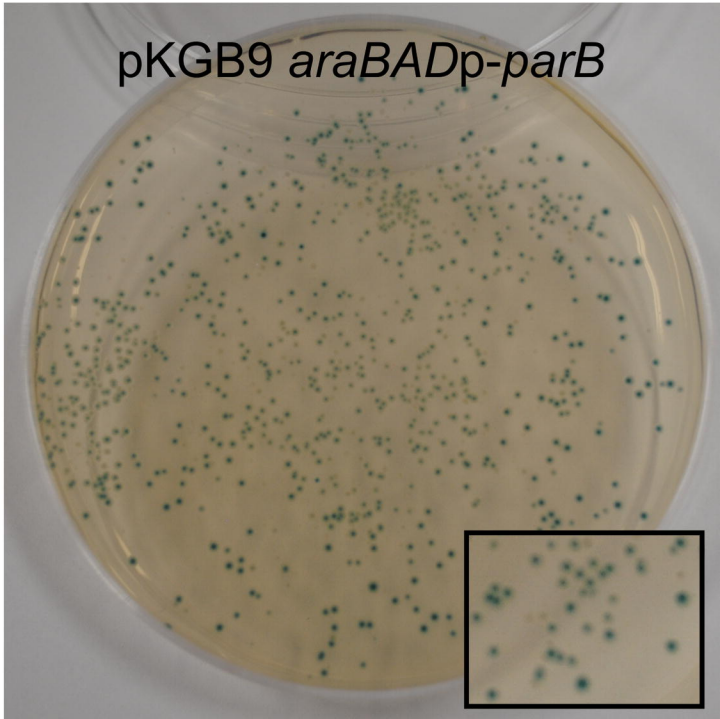

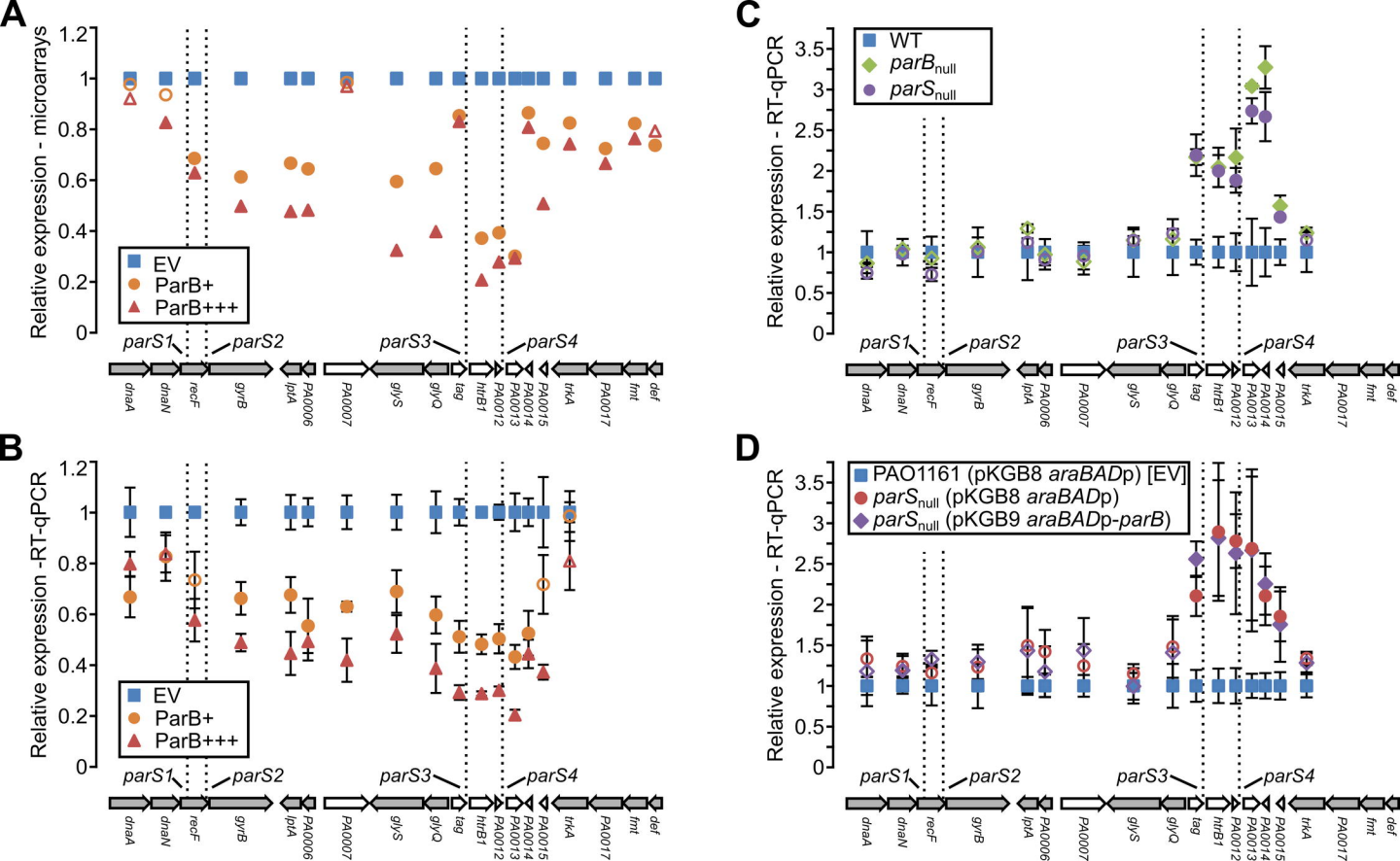
A
Relative expression - microarrays
EV
ParB+
ParB+++
parS1
parS2
parS3
parS4
dnaA
dnaN
recF
gyrB
lptA
PA0006
PA0007
glyS
glyQ
tag
hrB1
PA0012
PA0013
PA0014
PA0015
trkA
PA0017
fmt
def
B
Relative expression -RT-qPCR
EV
ParB+
ParB+++
C
Relative expression - RT-qPCR
WT
parB null
parS null
D
Relative expression - RT-qPCR
PAO1161 (pKGB8 araBADp) [EV]
parS null (pKGB8 araBADp)
parS null (pKGB9 araBADp-parB)

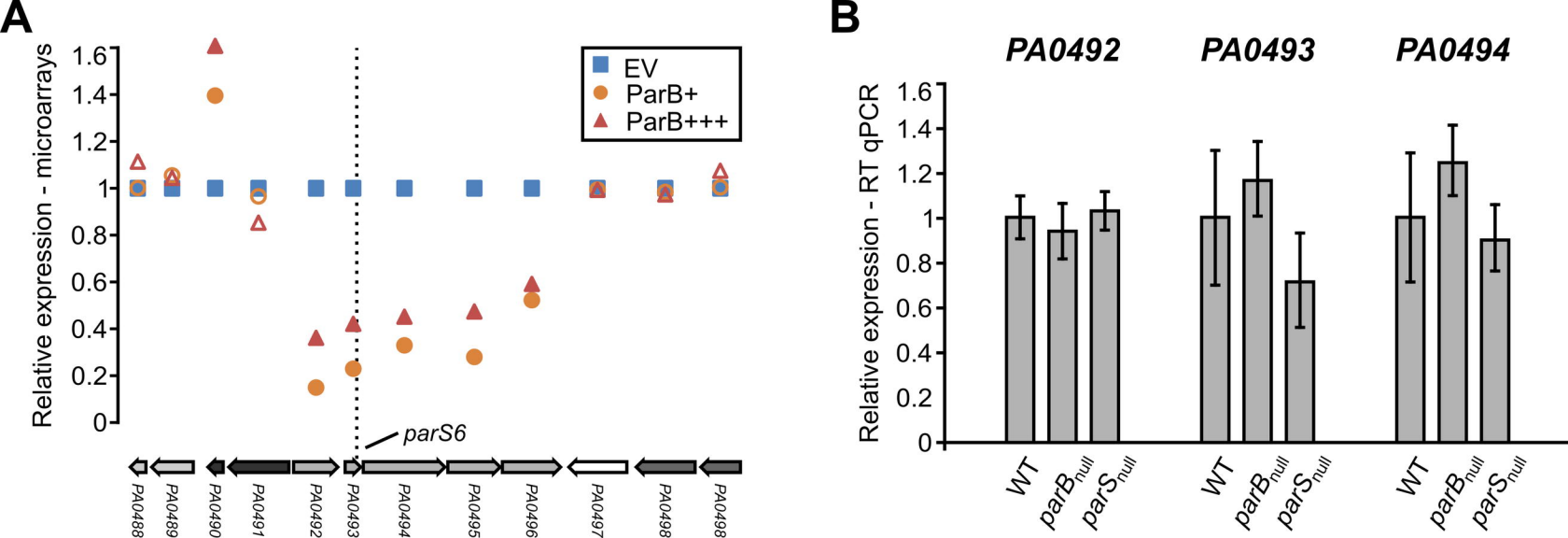
A
Relative expression - microarrays
1.6
1.4
1.2
1
0.8
0.6
0.4
0.2
0
EV
ParB+
ParB+++
parS6
PA0488
PA0489
PA0490
PA0491
PA0492
PA0493
PA0494
PA0495
PA0496
PA0497
PA0498
PA0498
B
PA0492
PA0493
PA0494
Relative expression - RT qPCR
1.6
1.4
1.2
1
0.8
0.6
0.4
0.2
0
WT
parB null
parS null
WT
parB null
parS null
WT
parB null
parS null

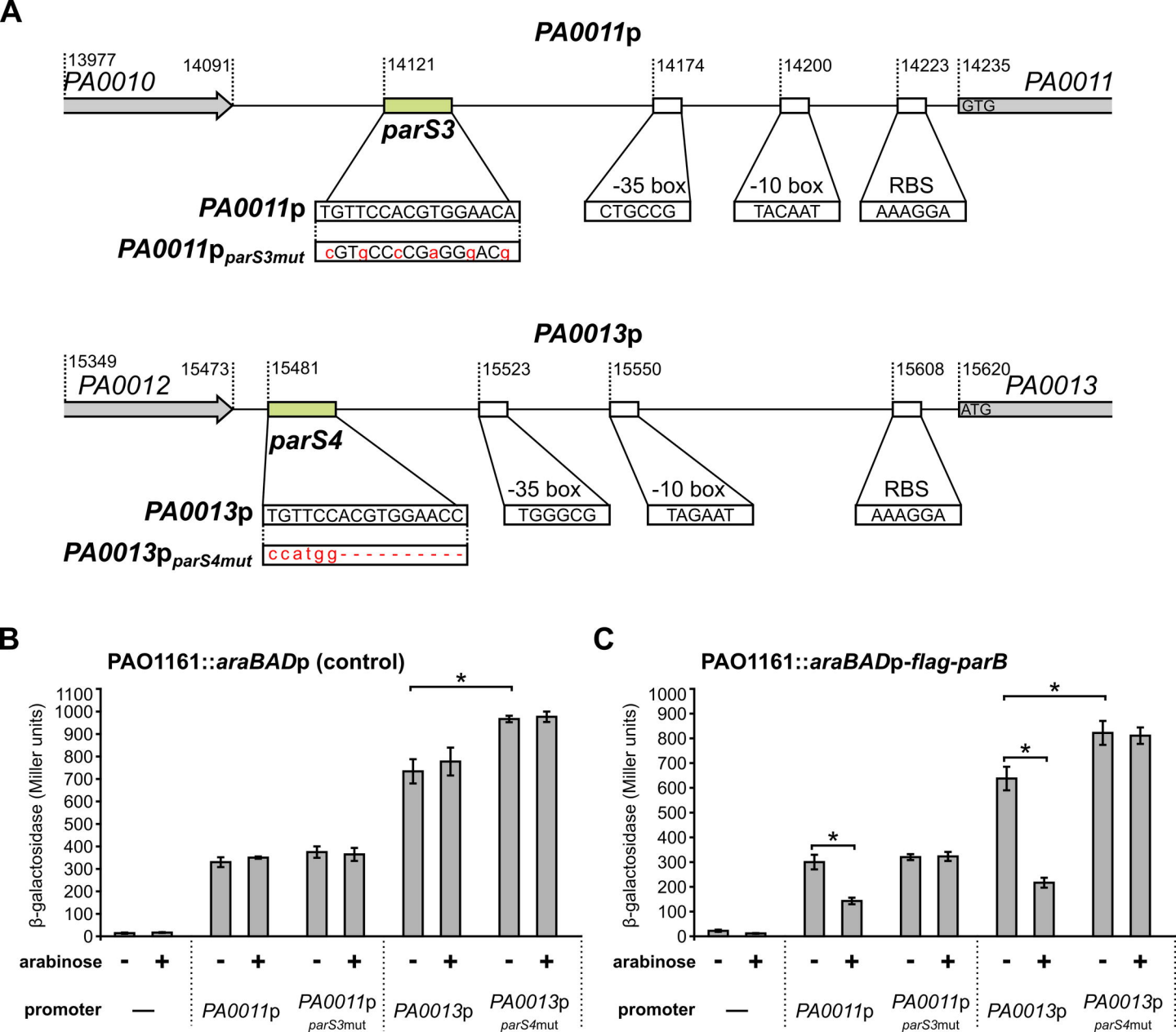
A
PA0011p
13977
PA0010
14091
14121
14174
14200
14223
14235
PA0011
GTG
parS3
-35 box
CTGCCG
-10 box
TACAAT
RBS
AAAGGA
PA0011p
TGTTCCACGTGGAACA
PA0011p parS3mut
cGTgCCcCGaGGgACg
PA0013p
15349
PA0012
15473
15481
15523
15550
15608
15620
PA0013
ATG
parS4
-35 box
TGGGCG
-10 box
TAGAAT
RBS
AAAGGA
PA0013p
TGTTCCACGTGGAACC
PA0013p parS4mut
ccatgg----------
B
PAO1161::araBADp (control)
β-galactosidase (Miller units)
1100
1000
900
800
700
600
500
400
300
200
100
0
*
arabinose - + - + - + - + - +
promoter — PA0011p PA0011p parS3mut PA0013p PA0013p parS4mut
C
PAO1161::araBADp-flag-parB
β-galactosidase (Miller units)
1000
900
800
700
600
500
400
300
200
100
0
*
*
*
arabinose - + - + - + - + - +
promoter — PA0011p PA0011p parS3mut PA0013p PA0013p parS4mut